



**AFRL-VA-WP-TP-2007-319**

**A FLEXIBLE HYPERSONIC VEHICLE MODEL  
DEVELOPED WITH PISTON THEORY (PREPRINT)**

**Michael W. Oppenheimer, Torstens Skujins, David B. Doman, and Michael A. Bolender**

**Control Design and Analysis Branch  
Structures Division**

**JULY 2007**

**Approved for public release; distribution unlimited.**

*See additional restrictions described on inside pages*

**STINFO COPY**

**AIR FORCE RESEARCH LABORATORY  
AIR VEHICLES DIRECTORATE  
WRIGHT-PATTERSON AIR FORCE BASE, OH 45433-7542  
AIR FORCE MATERIEL COMMAND  
UNITED STATES AIR FORCE**

## NOTICE AND SIGNATURE PAGE

Using Government drawings, specifications, or other data included in this document for any purpose other than Government procurement does not in any way obligate the U.S. Government. The fact that the Government formulated or supplied the drawings, specifications, or other data does not license the holder or any other person or corporation; or convey any rights or permission to manufacture, use, or sell any patented invention that may relate to them.

This report was cleared for public release by the Air Force Research Laboratory Wright Site (AFRL/WS) Public Affairs Office and is available to the general public, including foreign nationals. Copies may be obtained from the Defense Technical Information Center (DTIC) (<http://www.dtic.mil>).

AFRL-VA-WP-TP-2007-319 HAS BEEN REVIEWED AND IS APPROVED FOR PUBLICATION IN ACCORDANCE WITH ASSIGNED DISTRIBUTION STATEMENT.

\*//Signature//

---

Michael W. Oppenheimer  
Electronics Engineer  
Control Design and Analysis Branch  
Air Force Research Laboratory  
Air Vehicles Directorate

//Signature//

---

Deborah S. Grismer  
Chief  
Control Design and Analysis Branch  
Air Force Research Laboratory  
Air Vehicles Directorate

This report is published in the interest of scientific and technical information exchange, and its publication does not constitute the Government's approval or disapproval of its ideas or findings.

\*Disseminated copies will show “//Signature//” stamped or typed above the signature blocks.

<b>REPORT DOCUMENTATION PAGE</b>				<i>Form Approved</i> OMB No. 0704-0188	
<p>The public reporting burden for this collection of information is estimated to average 1 hour per response, including the time for reviewing instructions, searching existing data sources, gathering and maintaining the data needed, and completing and reviewing the collection of information. Send comments regarding this burden estimate or any other aspect of this collection of information, including suggestions for reducing this burden, to Department of Defense, Washington Headquarters Services, Directorate for Information Operations and Reports (0704-0188), 1215 Jefferson Davis Highway, Suite 1204, Arlington, VA 22202-4302. Respondents should be aware that notwithstanding any other provision of law, no person shall be subject to any penalty for failing to comply with a collection of information if it does not display a currently valid OMB control number. <b>PLEASE DO NOT RETURN YOUR FORM TO THE ABOVE ADDRESS.</b></p>					
<b>1. REPORT DATE (DD-MM-YY)</b> July 2007		<b>2. REPORT TYPE</b> Conference Paper Preprint		<b>3. DATES COVERED (From - To)</b> 01 September 2006 – 12 July 2007	
<b>4. TITLE AND SUBTITLE</b> A FLEXIBLE HYPERSONIC VEHICLE MODEL DEVELOPED WITH PISTON THEORY (PREPRINT)				<b>5a. CONTRACT NUMBER</b> In-house	
				<b>5b. GRANT NUMBER</b>	
				<b>5c. PROGRAM ELEMENT NUMBER</b> 62201F	
<b>6. AUTHOR(S)</b> Michael W. Oppenheimer, David B. Doman, and Michael A. Bolender (AFRL/VACA) Torstens Skujins (University of Michigan)				<b>5d. PROJECT NUMBER</b> A03G	
				<b>5e. TASK NUMBER</b>	
				<b>5f. WORK UNIT NUMBER</b> 0B	
<b>7. PERFORMING ORGANIZATION NAME(S) AND ADDRESS(ES)</b> Control Design and Analysis Branch, Structures Division Air Force Research Laboratory, Air Vehicles Directorate Wright-Patterson Air Force Base, OH 45433-7542 Air Force Materiel Command United States Air Force				University of Michigan	
<b>9. SPONSORING/MONITORING AGENCY NAME(S) AND ADDRESS(ES)</b>  Air Force Research Laboratory Air Vehicles Directorate Wright-Patterson Air Force Base, OH 45433-7542 Air Force Materiel Command United States Air Force				<b>10. SPONSORING/MONITORING AGENCY ACRONYM(S)</b> AFRL/VACA	
				<b>11. SPONSORING/MONITORING AGENCY REPORT NUMBER(S)</b> AFRL-VA-WP-TP-2007-319	
<b>12. DISTRIBUTION/AVAILABILITY STATEMENT</b> Approved for public release; distribution unlimited.					
<b>13. SUPPLEMENTARY NOTES</b> Conference paper submitted to the proceedings of the AIAA GNC Conference. The U.S. Government is joint author of this work and has the right to use, modify, reproduce, release, perform, display, or disclose the work. PAO Case Number: AFRL/WS 07-1763, 02 Aug 2007. Paper contains color.					
<b>14. ABSTRACT</b> For high Mach number flows, $M > 4$ , piston theory has been used to calculate the pressures on the surfaces of a vehicle. In a two-dimensional inviscid flow, a perpendicular column of fluid stays intact as it passes over a solid surface. Thus, the pressure at the surface can be calculated assuming the surface were a piston moving into a column of fluid. In this work, first-order piston theory is used to calculate the forces, moments, and stability derivatives for longitudinal motion of a hypersonic vehicle. Piston theory predicts a relationship between the local pressure on a surface and the normal component of fluid velocity produced by the surface's motion. The advantage of piston theory over other techniques, such as Prandtl-Meyer flow, oblique shock, or Newtonian impact theory, is that unsteady aerodynamic effects can be included in the model. The unsteady effects, considered in this work, include perturbations in the linear velocities and angular rates, due to rigid body motion. A flexible vehicle model is developed to take into account the aeroelastic behavior of the vehicle. The vehicle forebody and aftbody are modeled as cantilever beams fixed at the center-of-gravity. Piston theory is used to account for the changes in the forces and moments due to the flexing of the vehicle. Piston theory yields an analytical model for the longitudinal motion of the vehicle, thus allowing design trade studies to be performed while still providing insight into the physics of the problem.					
<b>15. SUBJECT TERMS</b> Piston Theory, Unsteady Aerodynamics, Aeroelastic Model					
<b>16. SECURITY CLASSIFICATION OF:</b>			<b>17. LIMITATION OF ABSTRACT:</b> SAR	<b>18. NUMBER OF PAGES</b> 32	<b>19a. NAME OF RESPONSIBLE PERSON (Monitor)</b> Michael W. Oppenheimer <b>19b. TELEPHONE NUMBER (Include Area Code)</b> N/A
<b>a. REPORT</b> Unclassified	<b>b. ABSTRACT</b> Unclassified	<b>c. THIS PAGE</b> Unclassified			

# A Flexible Hypersonic Vehicle Model Developed With Piston Theory

Michael W. Oppenheimer \*

Torstens Skujins †

David B. Doman ‡

Michael A. Bolender §

Air Force Research Laboratory, WPAFB, OH 45433-7531

## I. Abstract

For high Mach number flows,  $M \geq 4$ , piston theory has been used to calculate the pressures on the surfaces of a vehicle. In a two-dimensional inviscid flow, a perpendicular column of fluid stays intact as it passes over a solid surface. Thus, the pressure at the surface can be calculated assuming the surface were a piston moving into a column of fluid. In this work, first-order piston theory is used to calculate the forces, moments, and stability derivatives for longitudinal motion of a hypersonic vehicle. Piston theory predicts a relationship between the local pressure on a surface and the normal component of fluid velocity produced by the surface's motion. The advantage of piston theory over other techniques, such as Prandtl-Meyer flow, oblique shock, or Newtonian impact theory, is that unsteady aerodynamic effects can be included in the model. Prandtl-Meyer flow and oblique shock theory are utilized to provide flow properties over the surfaces of the vehicle. These flow properties are used to determine the steady forces and moments and are also included in the unsteady flow calculations. Thus, this work utilizes a combination of Prandtl-Meyer flow, oblique shock, and piston theory to calculate forces and moments. The unsteady effects, considered in this work, include perturbations in the linear velocities and angular rates, due to rigid body motion. A flexible vehicle model is developed to take into account the aeroelastic behavior of the vehicle. The vehicle forebody and aftbody are modelled as cantilever beams fixed at the center-of-gravity. Piston theory is used to account for the changes in the forces and moments due to the flexing of the vehicle. Piston theory yields an analytical model for the longitudinal motion of the vehicle, thus allowing design trade studies to be performed while still providing insight into the physics of the problem.

## II. Introduction

In the 1980's, the National Aerospace Plane (NASP) program commenced, with its goal being a feasibility study for a single-stage to orbit (SSTO) vehicle, which was reusable and could take off and land horizontally. The NASP was to be powered by a supersonic combustion ramjet (scramjet) engine. Although this program was cancelled in the 1990's, a great deal of knowledge was gained and it spawned future programs, including the hypersonic systems technology program (HySTP), initiated in late 1994, and the NASA X-43A. The HySTP's goal was to transfer the accomplishments of the NASP program to a technology demonstration program. This program was cancelled in early 1995. The NASA X-43A set new world speed records in 2004, reaching Mach 6.8 and Mach 9.6 on two separate occasions with a scramjet engine. These flights were the culmination of NASA's Hyper-X program, with the objective being to explore alternatives to rocket power for space access vehicles.

---

\*Electronics Engineer, Control Analysis and Design Branch, 2210 Eighth Street, Ste 21, Email Michael.Oppenheimer@wpafb.af.mil, Ph. (937) 255-8490, Fax (937) 656-4000, Member AIAA

†Graduate Student, University of Michigan, Email tsujins@umich.edu

‡Senior Aerospace Engineer, Control Analysis and Design Branch, 2210 Eighth Street, Ste 21, Email David.Doman@wpafb.af.mil, Ph. (937) 255-8451, Fax (937) 656-4000, Senior Member AIAA

§Aerospace Engineer, Control Analysis and Design Branch, 2210 Eighth Street, Ste 21, Email Michael.Bolender@wpafb.af.mil, Ph. (937) 255-8492, Fax (937) 656-4000, Senior Member AIAA

With renewed interest in space operations worldwide, there is an interest in hypersonic aerodynamics research. The scramjet engine will likely play a major role in future hypersonic vehicles. Unlike a conventional turbojet engine, a scramjet engine does not use high speed turbomachinery to compress the air before it reaches the combustor. Instead, it relies upon the rise in pressure across oblique shock waves located in front of the inlet. Furthermore, the flow through the entire engine is supersonic in contrast to a ramjet, where the flow speeds are subsonic through the combustor. On configurations like the NASP and X-43A, the underside of the airframe must function as the air inlet mechanism and the exhaust nozzle. Therefore, integration of the airframe and engine are critical to success of a scramjet powered vehicle.

Scramjets could be used as part of a multi-stage launch vehicle that would include multiple propulsion systems to perform a mission. The factor driving research towards scramjets and away from rockets is cost; scramjets would substantially lower costs because it is an airbreathing engine. Airbreathing engines don't require oxidizer to be carried by the vehicle, hence increasing the payload and reducing the quantity of fuel carried.

Unsteady aerodynamics are a phenomenon that must be considered in the development and optimization of future hypersonic vehicles. The combined effects of a slender flexible vehicle travelling at high speeds and subjected to large forces may lead to significant unsteady aerodynamic effects. Hence, understanding the concepts and consequences of time-dependent aerodynamic flows is critical to the successful development of this type of vehicle.

Piston theory is a technique that has been used for years to determine the pressure distributions on an airfoil/vehicle, when the Mach number is sufficiently high. Lighthill<sup>1</sup> discussed the application of piston theory on oscillating airfoils some 50 years ago. Ashley and Zartarian<sup>2</sup> discuss piston theory while providing a number of examples of the application of piston theory to specific problems. More recently, Tarpley<sup>3</sup> discussed the computation of stability derivatives for a caret-wing waverider using piston theory, which requires the analysis of unsteady flow over the vehicle. Piston theory allows the inclusion of unsteady aerodynamic effects in the model and a closed form solution can be found for these unsteady effects.

In this work, piston theory is applied to a hypothetical 2-dimensional hypersonic vehicle powered with a scramjet. This work uses first-order piston theory to compute unsteady effects behind shock waves and expansion fans. A recent study<sup>4</sup> revealed that this method of computing unsteady aerodynamic effects delivered highly accurate results when compared to computational fluid dynamics solutions and higher order piston theory models. This paper builds on previous work<sup>5</sup> by incorporating a flexible vehicle model and determining the perturbations to forces and moments due to flexibility.

In Section III, the vehicle analyzed in this work is described, while the steady forces and pressures on the vehicle's surfaces are provided in Section IV. The unsteady effects due to the aerodynamic control surfaces are included in Section V, the total rigid body forces and moments are discussed in Section VI, while the aeroelastic model is developed in Section VII. Results are provided in Section VIII, conclusions are given in Section IX, and Appendix A contains detailed calculations for many of the flexible stability derivatives.

### III. HSV Model

Figure 1 shows the 2-dimensional hypersonic vehicle considered in this work.<sup>6</sup> The longitudinal force and moment analysis is taken as unit depth into the page. The vehicle consists of 4 surfaces: an upper surface (defined by points cf) and three lower surfaces (defined by points cd, gh, and ef). All pertinent lengths and dimensions are in units of feet and degrees, respectively. The total length of the vehicle is  $L = 100ft$  and the notation for lengths is  $L_f =$  length of the forebody,  $L_n =$  length of the engine nacelle,  $L_a =$  length of the aftbody,  $L_e$  is the length of the elevator,  $L_c$  is the length of the canard,  $\bar{x}_f$  is the distance from the C.G. to the front of the vehicle,  $\bar{x}_a$  is the distance from the C.G. to the rear of the vehicle,  $x_{elev}$  and  $z_{elev}$  are the distances from the C.G. to the midpoint of the elevator in the x and z directions, respectively,  $x_{canard}$  is the distance from the C.G. to the midpoint of the canard, and  $h_i$  is the engine height. The vehicle dimensions

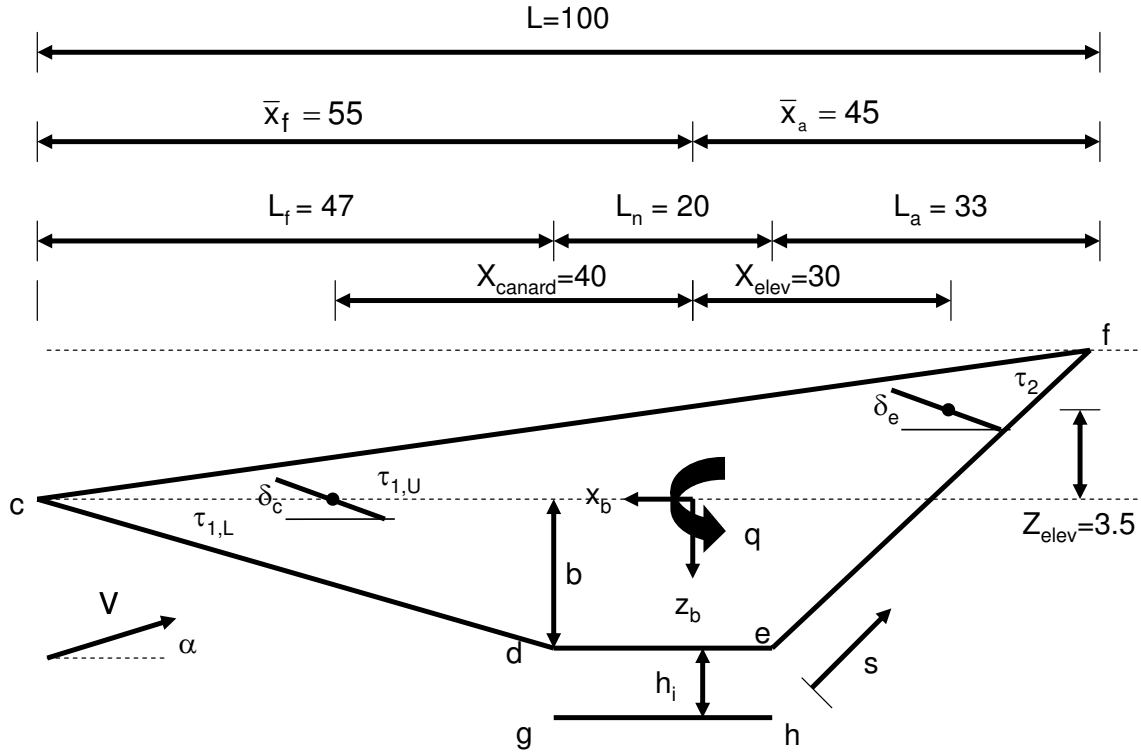


Figure 1. Hypersonic Vehicle.

are

$$\begin{aligned}
 L &= 100 \text{ ft} \\
 L_f &= 47 \text{ ft} \\
 L_a &= 33 \text{ ft} \\
 L_n &= 20 \text{ ft} \\
 L_e &= 17 \text{ ft} \\
 L_c &= 10 \text{ ft} \\
 \bar{x}_f &= 55 \text{ ft} \\
 \bar{x}_a &= 45 \text{ ft} \\
 x_{elev} &= 30 \text{ ft} \\
 z_{elev} &= 3.5 \text{ ft} \\
 h_i &= 3.25 \text{ ft} \\
 x_{canard} &= 40 \text{ ft}
 \end{aligned} \tag{1}$$

The vehicle angles are

$$\begin{aligned}
 \tau_{1,U} &= 3^\circ \\
 \tau_{1,L} &= 6^\circ \\
 \tau_2 &= 14.41^\circ
 \end{aligned} \tag{2}$$

Additionally, the vehicle mass and moment of inertia are

$$\begin{aligned}
 Mass &= 300 \frac{\text{slug}}{\text{ft}} \\
 J_{yy} &= 500,000 \frac{\text{slug-ft}^2}{\text{ft}}
 \end{aligned} \tag{3}$$

and the mean aerodynamic chord ( $\bar{c}$ ) and planform area ( $S$ ) are defined as

$$\begin{aligned}\bar{c} &= L \\ S &= L^2\end{aligned}\tag{4}$$

The goal is to apply piston theory to this 2-dimensional vehicle geometry to determine the pressure distribution on the surfaces of the vehicle, which, in turn, can be used to evaluate the forces and moments. The pressure on the face of a piston moving into a column of perfect gas is<sup>2</sup>

$$\frac{P}{P_\infty} = \left(1 + \frac{\gamma - 1}{2} \frac{V_n}{a_\infty}\right)^{\frac{2\gamma}{\gamma - 1}}\tag{5}$$

where the subscript "∞" refers to the steady flow conditions past the surface,  $V_n$  is the velocity of the surface normal to the steady flow,  $a_\infty$  is the freestream speed of sound, and  $P$  is the surface pressure. Taking the binomial expansion of Eq. 5, to first order, produces

$$\frac{P}{P_\infty} = 1 + \frac{2\gamma}{\gamma - 1} \frac{\gamma - 1}{2} \frac{V_n}{a_\infty} = 1 + \frac{\gamma V_n}{a_\infty}\tag{6}$$

Multiplying through by  $P_\infty$  and using the perfect gas law ( $P = \rho RT$ ) and the definition of the speed of sound ( $a^2 = \gamma RT$ ) yields the basic result from first-order linear piston theory

$$P = P_\infty + \rho_\infty a_\infty V_n\tag{7}$$

where  $\gamma$  is the ratio of specific heats and  $R$  is the gas constant. The infinitesimal force, on an elemental area, due to the pressure is given by

$$d\mathbf{F} = -Pd\mathbf{A}\mathbf{n}\tag{8}$$

where  $dA$  is a surface element and  $\mathbf{n}$  is the outward pointing normal. Substituting Eq. 7 into Eq. 8 yields

$$d\mathbf{F} = (-P_\infty - \rho_\infty a_\infty V_n) d\mathbf{A}\mathbf{n}\tag{9}$$

The normal velocity can be computed by taking the dot product of the flow velocity over a surface and the outward pointing normal for that surface. Hence, Eq. 9 becomes

$$d\mathbf{F} = (-P_\infty - \rho_\infty a_\infty [\mathbf{V} \cdot \mathbf{n}]) d\mathbf{A}\mathbf{n}\tag{10}$$

Equation 10 is the basic result upon which this work is based. From this equation, it is seen that in order to compute the forces acting on a surface, one must determine the properties of the flow past the surface (properties behind a shock, expansion fan, or freestream), the velocity of the surface relative to the airstream,  $\mathbf{V}$ , the outward pointing surface normal,  $\mathbf{n}$ , and the surface element,  $dA$ . The work that follows will develop these quantities for the upper and lower surfaces of the vehicle, as well as for the control effectors.

#### IV. Vehicle Surface Pressure Distributions and Forces

The differential forces on the surfaces of the vehicle were computed by Oppenheimer and Doman<sup>5</sup> and are repeated below:

$$d\mathbf{F}_{cf} = (-P_{cf} - \rho_{cf}a_{cf} \{[u + q \tan \tau_{1,U} (x - \bar{x}_f)] \sin \tau_{1,U} - [w - qx] \cos \tau_{1,U}\}) \left[ \sin \tau_{1,U} \hat{i} - \cos \tau_{1,U} \hat{k} \right] \sec \tau_{1,U} dx\tag{11}$$

$$d\mathbf{F}_{cd} = (-P_{cd} - \rho_{cd}a_{cd} \{[u - q \tan \tau_{1,L} (x - \bar{x}_f)] \sin \tau_{1,L} + [w - qx] \cos \tau_{1,L}\}) \left[ \sin \tau_{1,L} \hat{i} + \cos \tau_{1,L} \hat{k} \right] \sec \tau_{1,L} dx\tag{12}$$

$$d\mathbf{F}_{gh} = (-P_{gh} - \rho_{gh}a_{gh} \{w - qx\}) \left[ 1 \hat{k} \right] dx\tag{13}$$

$$d\mathbf{F}_{ef} = (-P_{ef} - \rho_{ef}a_{ef} \{-(u + qr_{efz}) \sin (\tau_{1,U} + \tau_2) + (w - qx) \cos (\tau_{1,U} + \tau_2)\}) \mathbf{n}_{ef} \sec (\tau_{1,U} + \tau_2) dx\tag{14}$$

where

$$\mathbf{n}_{ef} = -\sin(\tau_{1,U} + \tau_2) \hat{i} + \cos(\tau_{1,U} + \tau_2) \hat{k} \quad (15)$$

and

$$r_{efz} = [\tan(\tau_{1,U} + \tau_2)(x + \bar{x}_a) - L \tan \tau_{1,U}] \quad (16)$$

where  $u$ ,  $w$ , and  $q$  are small perturbations in a steady flight condition of the forward velocity, normal velocity, and pitch rate, respectively. The steady forces are computed by integrating the steady components of the differential forces over the corresponding surface. Performing the integrations yields

$$\begin{aligned} \mathbf{F}_{cf_a} &= -P_{cf} \bar{x}_a \sec \tau_{1,U} \left[ \sin \tau_{1,U} \hat{i} - \cos \tau_{1,U} \hat{k} \right] = X_{cf_a} \hat{i} + Z_{cf_a} \hat{k} \\ \mathbf{F}_{cf_f} &= -P_{cf} \bar{x}_f \sec \tau_{1,U} \left[ \sin \tau_{1,U} \hat{i} - \cos \tau_{1,U} \hat{k} \right] = X_{cf_f} \hat{i} + Z_{cf_f} \hat{k} \end{aligned} \quad (17)$$

where  $X_{cf_a}$ ,  $Z_{cf_a}$  are the components of the aftbody upper surface force in the x and z directions, respectively, and  $X_{cf_f}$ ,  $Z_{cf_f}$  are the components of the forebody upper surface force in the x and z directions. The lower surface forces are

$$\begin{aligned} \mathbf{F}_{cd} &= -P_{cd} L_f \sec \tau_{1,L} \left[ \sin \tau_{1,L} \hat{i} + \cos \tau_{1,L} \hat{k} \right] = X_{cd} \hat{i} + Z_{cd} \hat{k} \\ \mathbf{F}_{gh} &= -P_{gh} L_n \hat{k} = X_{gh} \hat{i} + Z_{gh} \hat{k} \end{aligned} \quad (18)$$

while on the rear ramp, the vector force due to the external nozzle is

$$\mathbf{F}_{ef} = \frac{L_a P_e P_\infty}{\cos(\tau_{1,U} + \tau_2)(P_e - P_\infty)} \ln \frac{P_e}{P_\infty} \left[ \sin(\tau_{1,U} + \tau_2) \hat{i} - \cos(\tau_{1,U} + \tau_2) \hat{k} \right] = X_{ef} \hat{i} + Z_{ef} \hat{k} \quad (19)$$

where  $X_{ef}$  and  $Z_{ef}$  are the axial and normal force components of the external nozzle force and  $P_e$  is the engine exit pressure.

## A. Control Surfaces

The control surfaces are an elevator and canard as shown in Fig. 1. Both surfaces are modelled as flat plates hinged at their midpoints so the entire surface deflects. Positive deflection is defined as trailing edge down. The x and z positions of the midpoint of the elevator and canard referenced to the C.G. are  $x_{elev}$ ,  $z_{elev}$  and  $x_{canard}$ , 0. The canard was added to this vehicle for two reasons. First, the elevator produces a significant amount of lift and results in a non-minimum phase flight path angle response.<sup>7</sup> Adding the canard and forcing it to respond in conjunction with the elevator compensates for the lift produced by the elevator and reduces the non-minimum phase behavior. Secondly, the canard can be utilized for low speed control and reduces the takeoff and landing speeds since they produce positive lift in conjunction with a nose up pitching moment. In this work, the canard is not ganged to the elevator, rather, it is free to move. Hence, the non-minimum phase flight path angle response is still present. However, this allows the determination of the steady and unsteady forces and moments due to the canard.

### 1. Elevator

The upper and lower forces on the elevator can be computed as

$$\mathbf{F}_{eU} = \int_{-x_{elev} - \frac{L_e}{2} \cos \delta_e}^{-x_{elev} + \frac{L_e}{2} \cos \delta_e} [-P_{eU} - \rho_{eU} a_{eU} \{\mathbf{V}_{eU} \cdot \mathbf{n}_{eU}\}] \left[ -\sin \delta_e \hat{i} - \cos \delta_e \hat{k} \right] \sec \delta_e dx \quad (20)$$

$$\mathbf{F}_{eL} = \int_{-x_{elev} - \frac{L_e}{2} \cos \delta_e}^{-x_{elev} + \frac{L_e}{2} \cos \delta_e} [-P_{eL} - \rho_{eL} a_{eL} \{\mathbf{V}_{eL} \cdot \mathbf{n}_{eL}\}] \left[ \sin \delta_e \hat{i} + \cos \delta_e \hat{k} \right] \sec \delta_e dx \quad (21)$$

where

$$\mathbf{V}_{eU} \cdot \mathbf{n}_{eU} = -(u - q \{z_{elev} + \tan \delta_e (x + x_{elev})\}) \sin \delta_e - (w - qx) \cos \delta_e \quad (22)$$

$$\mathbf{V}_{eL} \cdot \mathbf{n}_{eL} = (u - q \{z_{elev} + \tan \delta_e (x + x_{elev})\}) \sin \delta_e + (w - qx) \cos \delta_e \quad (23)$$

## 2. Canard

In order to determine the steady and unsteady forces and moments due to the canard, Eq. 10 must be evaluated. Hence, the flow properties on the top and bottom surfaces of the canard along with a position vector, normal vector, and surface element must be determined. For the canard, the flow properties are

$$\begin{aligned}
 & \text{If } \delta_c = -\alpha \implies \text{Freestream} \\
 & \text{If } \delta_c < -\alpha \implies \text{Shock on top, expansion on bottom} \\
 & \text{If } \delta_c > -\alpha \implies \text{Expansion on top, shock on bottom}
 \end{aligned} \tag{24}$$

The position vector from the C.G. to an arbitrary point on the canard is given by

$$\begin{aligned}
 \mathbf{r}_c &= x\hat{i} + [-\tan \delta_c (x - x_{canard}) + z_{canard}] \\
 x_{canard} - \frac{L_c}{2} \cos \delta_c &\leq x \leq x_{canard} + \frac{L_c}{2} \cos \delta_c
 \end{aligned} \tag{25}$$

where  $z_{canard} = 0$  for this configuration. The outward pointing normal vectors for this surface, relative to the body axis, are

$$\begin{aligned}
 \mathbf{n}_{cU} &= -\sin \delta_c \hat{i} - \cos \delta_c \hat{k} \\
 \mathbf{n}_{cL} &= \sin \delta_c \hat{i} + \cos \delta_c \hat{k}
 \end{aligned} \tag{26}$$

and the surface element is

$$dA_c = \sec \delta_c (1) dx \tag{27}$$

To compute the forces, moments, and stability derivatives, consider small perturbations, from a steady flight condition, in the velocities  $u$  and  $w$  and the pitch rate  $q$ . The velocity of a point on the upper and lower surfaces of the canard, due to these perturbations, is

$$\begin{aligned}
 \mathbf{V}_{cU} &= (V_{cU} \cos \delta_c + u) \hat{i} + (-V_{cU} \sin \delta_c + w) \hat{k} + \boldsymbol{\omega} \times \mathbf{r}_c \\
 \mathbf{V}_{cL} &= (V_{cL} \cos \delta_c + u) \hat{i} + (-V_{cL} \sin \delta_c + w) \hat{k} + \boldsymbol{\omega} \times \mathbf{r}_c
 \end{aligned} \tag{28}$$

where  $V_{cU}$  and  $V_{cL}$  are the flow velocities on the upper and lower surface of the canard (as determined from the flow analysis) and  $\boldsymbol{\omega} = q\hat{j}$  is the angular rate vector. Using Eqs. 24 - 28 in Eq. 10 yields the differential forces due to the canard:

$$\begin{aligned}
 d\mathbf{F}_{cU} &= [-P_{cU} - \rho_{cU} a_{cU} \{-\sin \delta_c (u + q[-\tan \delta_c (x - x_{canard}) + z_{canard}]) - \cos \delta_c (w - qz)\}] \mathbf{n}_{cU} dA_{cU} \\
 d\mathbf{F}_{cL} &= [-P_{cL} - \rho_{cL} a_{cL} \{\sin \delta_c (u + q[-\tan \delta_c (x - x_{canard}) + z_{canard}]) + \cos \delta_c (w - qz)\}] \mathbf{n}_{cL} dA_{cL}
 \end{aligned} \tag{29}$$

The steady forces are computed by integrating the steady component of Eq. 29, hence,

$$\begin{aligned}
 \mathbf{F}_{cU} &= \int_{x_{canard} - \frac{L_c}{2} \cos \delta_c}^{x_{canard} + \frac{L_c}{2} \cos \delta_c} -P_{cU} \left( -\sin \delta_c \hat{i} - \cos \delta_c \hat{k} \right) \sec \delta_c dx = P_{cU} L_c \sin \delta_c \hat{i} + P_{cU} L_c \cos \delta_c \hat{k} = X_{cU} \hat{i} + Z_{cU} \hat{k} \\
 \mathbf{F}_{cL} &= \int_{x_{canard} - \frac{L_c}{2} \cos \delta_c}^{x_{canard} + \frac{L_c}{2} \cos \delta_c} -P_{cL} \left( \sin \delta_c \hat{i} + \cos \delta_c \hat{k} \right) \sec \delta_c dx = -P_{cL} L_c \sin \delta_c \hat{i} - P_{cL} L_c \cos \delta_c \hat{k} = X_{cL} \hat{i} + Z_{cL} \hat{k}
 \end{aligned} \tag{30}$$

The corresponding moments are calculated using  $M_{cU} = \mathbf{r}_c \times \mathbf{F}_{cU}$  and  $M_{cL} = \mathbf{r}_c \times \mathbf{F}_{cL}$  such that

$$\begin{aligned}
 M_{cU} &= -x_{canard} P_{cU} L_c \cos \delta_c + z_{canard} P_{cU} L_c \sin \delta_c = -x_{canard} P_{cU} L_c \cos \delta_c \\
 M_{cL} &= x_{canard} P_{cL} L_c \cos \delta_c - z_{canard} P_{cL} L_c \sin \delta_c = x_{canard} P_{cL} L_c \cos \delta_c
 \end{aligned} \tag{31}$$

where the last inequalities in Eq. 31 result from  $z_{canard}$  being zero.

## V. Unsteady Control Surface Effects

The unsteady effects due to velocity and rate perturbations on the control surfaces are found using the unsteady portions of Eqs. 20, 21, and 29.

## A. Elevator Unsteady Effects

The normal force stability derivative due to the elevator is

$$(C_{Z_w})_{\delta_e} = \frac{1}{q_\infty S} \int (d\mathbf{F})_{z-w} = \frac{1}{q_\infty S} \int (d\mathbf{F}_{e_U})_{z-w} + \frac{1}{q_\infty S} \int (d\mathbf{F}_{e_L})_{z-w} \quad (32)$$

Performing the necessary substitutions produces

$$(C_{Z_w})_{\delta_e} = \frac{1}{q_\infty S} \left[ \int_{-x_{elev} - \frac{L_e}{2} \cos \delta_e}^{-x_{elev} + \frac{L_e}{2} \cos \delta_e} -\rho_{e_U} a_{e_U} w \cos \delta_e dx + \int_{-x_{elev} - \frac{L_e}{2} \cos \delta_e}^{-x_{elev} + \frac{L_e}{2} \cos \delta_e} -\rho_{e_L} a_{e_L} w \cos \delta_e dx \right] \quad (33)$$

Integrating, letting  $w \approx V_\infty \alpha$ , and simplifying yields

$$\left( \frac{\partial C_Z}{\partial \alpha} \right)_{\delta_e} = \frac{-(\rho_{e_U} a_{e_U} + \rho_{e_L} a_{e_L}) V_\infty L_e \cos^2 \delta_e}{q_\infty S} \quad (34)$$

Using similar analysis, the axial force component becomes

$$\begin{aligned} (C_{X_w})_{\delta_e} &= \frac{1}{q_\infty S} \int (d\mathbf{F})_{x-w} = \frac{1}{q_\infty S} \int (d\mathbf{F}_{e_U})_{x-w} + \frac{1}{q_\infty S} \int (d\mathbf{F}_{e_L})_{x-w} \\ &\Rightarrow \left( \frac{\partial C_X}{\partial \alpha} \right)_{\delta_e} = \frac{-(\rho_{e_U} a_{e_U} + \rho_{e_L} a_{e_L}) V_\infty L_e \cos \delta_e \sin \delta_e}{q_\infty S} \end{aligned} \quad (35)$$

The pitching moment contribution due to w motion is

$$\begin{aligned} (C_{M_w})_{\delta_e} &= \frac{1}{q_\infty S \bar{c}} \left[ \int z (d\mathbf{F}_{e_U})_{x-w} + \int z (d\mathbf{F}_{e_L})_{x-w} - \int x (d\mathbf{F}_{e_U})_{z-w} - \int x (d\mathbf{F}_{e_L})_{z-w} \right] \\ &\Rightarrow \left( \frac{\partial C_M}{\partial \alpha} \right)_{\delta_e} = \frac{(\rho_{e_U} a_{e_U} + \rho_{e_L} a_{e_L}) (z_{elev} L_e \sin \delta_e \cos \delta_e - x_{elev} L_e \cos^2 \delta_e) V_\infty}{q_\infty S \bar{c}} \end{aligned} \quad (36)$$

The normal force increment due to pitch rate is

$$\begin{aligned} (C_{Z_q})_{\delta_e} &= \frac{1}{q_\infty S} \left[ \int (d\mathbf{F}_{e_U})_{z-q} + \int (d\mathbf{F}_{e_L})_{z-q} \right] \\ &\Rightarrow \left( \frac{\partial C_Z}{\partial q} \right)_{\delta_e} = \frac{(\rho_{e_U} a_{e_U} + \rho_{e_L} a_{e_L}) [L_e \sin \delta_e \cos \delta_e \{z_{elev} + x_{elev} \tan \delta_e\} - x_{elev} L_e]}{q_\infty S} \end{aligned} \quad (37)$$

The final stability derivative for the elevator is the pitching moment increment due to pitch rate, which becomes

$$(C_{M_q})_{\delta_e} = \frac{1}{q_\infty S \bar{c}} \left[ \int z (d\mathbf{F}_{e_U})_{x-q} + \int z (d\mathbf{F}_{e_L})_{x-q} - \int x (d\mathbf{F}_{e_U})_{z-q} - \int x (d\mathbf{F}_{e_L})_{z-q} \right] \quad (38)$$

Performing the required operations yields

$$\begin{aligned} \left( \frac{\partial C_M}{\partial q} \right)_{\delta_e} &= \frac{(\rho_{e_U} a_{e_U} + \rho_{e_L} a_{e_L})}{q_\infty S \bar{c}} [L_e \sin \delta_e \cos \delta_e (\tan \delta_e \{x_{elev}^2 - z_{elev}^2\} + x_{elev} z_{elev} \{1 - \tan^2 \delta_e\})] \\ &\quad + \frac{(\rho_{e_U} a_{e_U} + \rho_{e_L} a_{e_L})}{q_\infty S \bar{c}} (z_{elev} + x_{elev} \tan \delta_e) x_{elev} L_e \tan \delta_e \\ &\quad - \frac{(\rho_{e_U} a_{e_U} + \rho_{e_L} a_{e_L})}{q_\infty S \bar{c}} \left( \frac{\tan^2 \delta_e - 1}{3 \cos \delta_e} \right) \left( \left\{ -x_{elev} + \frac{L_e}{2} \cos \delta_e \right\}^3 - \left\{ -x_{elev} - \frac{L_e}{2} \cos \delta_e \right\}^3 \right) \end{aligned} \quad (39)$$

## B. Canard Unsteady Effects

The normal force stability derivative due to the canard is

$$(C_{Z_w})_{\delta_c} = \frac{1}{q_\infty S} \int (d\mathbf{F}_{c_U})_{z-w} + \frac{1}{q_\infty S} \int (d\mathbf{F}_{c_L})_{z-w} \quad (40)$$

which becomes

$$\left(\frac{\partial C_Z}{\partial \alpha}\right)_{\delta_c} = -\frac{(\rho_{c_U} a_{c_U} + \rho_{c_L} a_{c_L})(V_\infty L_c \cos^2 \delta_c)}{q_\infty S} \quad (41)$$

The axial force increment due to motion in the vertical direction becomes

$$\begin{aligned} (C_{X_w})_{\delta_c} &= \frac{1}{q_\infty S} \int (d\mathbf{F}_{c_U})_{x-w} + \frac{1}{q_\infty S} \int (d\mathbf{F}_{c_L})_{x-w} \\ \Rightarrow \left(\frac{\partial C_X}{\partial \alpha}\right)_{\delta_c} &= \frac{-(\rho_{c_U} a_{c_U} + \rho_{c_L} a_{c_L}) V_\infty L_c \cos \delta_c \sin \delta_c}{q_\infty S} \end{aligned} \quad (42)$$

The pitching moment contribution due to w motion is

$$\begin{aligned} (C_{M_w})_{\delta_c} &= \frac{1}{q_\infty S \bar{c}} \left[ \int z (d\mathbf{F}_{c_U})_{x-w} + \int z (d\mathbf{F}_{c_L})_{x-w} - \int x (d\mathbf{F}_{c_U})_{z-w} - \int x (d\mathbf{F}_{c_L})_{z-w} \right] \\ \Rightarrow \left(\frac{\partial C_M}{\partial \alpha}\right)_{\delta_c} &= \frac{(\rho_{c_U} a_{c_U} + \rho_{c_L} a_{c_L}) (-z_{canard} L_c \sin \delta_c \cos \delta_c + x_{canard} L_c \cos^2 \delta_c) V_\infty}{q_\infty S \bar{c}} \end{aligned} \quad (43)$$

The normal force increment due to pitch rate is

$$\begin{aligned} (C_{Z_q})_{\delta_c} &= \frac{1}{q_\infty S} \left[ \int (d\mathbf{F}_{c_U})_{z-q} + \int (d\mathbf{F}_{c_L})_{z-q} \right] \\ \Rightarrow \left(\frac{\partial C_Z}{\partial q}\right)_{\delta_c} &= \frac{(\rho_{c_U} a_{c_U} + \rho_{c_L} a_{c_L}) [x_{canard} L_c \cos^2 \delta_c - z_{canard} L_c \sin \delta_c \cos \delta_c]}{q_\infty S} \end{aligned} \quad (44)$$

The final stability derivative for the canard is the pitching moment increment due to pitch rate, which becomes

$$(C_{M_q})_{\delta_c} = \frac{1}{q_\infty S \bar{c}} \left[ \int z (d\mathbf{F}_{c_U})_{x-q} + \int z (d\mathbf{F}_{c_L})_{x-q} - \int x (d\mathbf{F}_{c_U})_{z-q} - \int x (d\mathbf{F}_{c_L})_{z-q} \right] \quad (45)$$

Performing the required operations yields

$$\left(\frac{\partial C_M}{\partial q}\right)_{\delta_c} = \frac{(\rho_{c_U} a_{c_U} + \rho_{c_L} a_{c_L})}{q_\infty S \bar{c}} \left[ -\frac{\sin^2 \delta_c L_c^3}{12} - z_{canard}^2 L_c \sin^2 \delta_c - \frac{L_c^3}{12} \sin^2 \delta_c \cos^2 \delta_c - x_{canard}^2 L_c \cos^2 \delta_c - \frac{L_c^3 \cos^4 \delta_c}{12} \right] \quad (46)$$

## VI. Total Forces and Moments - Rigid Body

With the inclusion of the stability derivatives, the thrust, and resulting engine moment,<sup>5</sup> the total aerodynamic forces and moments on the vehicle are

$$\begin{aligned} X_{total} &= X_{c_{f_f}} + X_{c_{f_a}} + X_{c_d} + X_{gh} + X_{e_f} + X_{e_L} + X_{e_U} + X_{c_U} + X_{c_L} + T + q_\infty S \frac{\partial C_X}{\partial \alpha} \alpha \\ &\quad + q_\infty S \left(\frac{\partial C_X}{\partial \alpha}\right)_{\delta_e} \alpha + q_\infty S \left(\frac{\partial C_X}{\partial \alpha}\right)_{\delta_c} \alpha \end{aligned} \quad (47)$$

$$\begin{aligned} Z_{total} &= Z_{c_{f_f}} + Z_{c_{f_a}} + Z_{c_d} + Z_{gh} + Z_{e_f} + Z_{e_L} + Z_{e_U} + Z_{c_U} + Z_{c_L} + q_\infty S \frac{\partial C_Z}{\partial \alpha} \alpha + q_\infty S \frac{\partial C_Z}{\partial q} \frac{q\bar{c}}{2V_\infty} \\ &\quad + q_\infty S \left(\frac{\partial C_Z}{\partial \alpha}\right)_{\delta_e} \alpha + q_\infty S \left(\frac{\partial C_Z}{\partial \alpha}\right)_{\delta_c} \alpha + q_\infty S \left(\frac{\partial C_Z}{\partial q}\right)_{\delta_e} \frac{q\bar{c}}{2V_\infty} + q_\infty S \left(\frac{\partial C_Z}{\partial q}\right)_{\delta_c} \frac{q\bar{c}}{2V_\infty} \end{aligned} \quad (48)$$

$$\begin{aligned} M_{total} &= M_{c_{f_f}} + M_{c_{f_a}} + M_{c_d} + M_{gh} + M_{e_f} + M_{e_L} + M_{e_U} + M_{c_U} + M_{c_L} + M_{engine} + q_\infty S \bar{c} \frac{\partial C_M}{\partial \alpha} \alpha + \\ &\quad q_\infty S \bar{c} \frac{\partial C_M}{\partial q} \frac{q\bar{c}}{2V_\infty} + q_\infty S \bar{c} \left(\frac{\partial C_M}{\partial \alpha}\right)_{\delta_e} \alpha + q_\infty S \bar{c} \left(\frac{\partial C_M}{\partial \alpha}\right)_{\delta_c} \alpha + q_\infty S \bar{c} \left(\frac{\partial C_M}{\partial q}\right)_{\delta_e} \frac{q\bar{c}}{2V_\infty} + q_\infty S \bar{c} \left(\frac{\partial C_M}{\partial q}\right)_{\delta_c} \frac{q\bar{c}}{2V_\infty} \end{aligned} \quad (49)$$

where  $M_{engine}$  and  $T$  are the moment and thrust produced by the engine. It can be seen that Eqs. 47- 49 do not contain any inlet turning forces/moments that was present in previous work. Here, a reflected shock from the engine inlet was modelled and performs the flow turning.

## VII. Flexible Effects

Thus far, only unsteady effects due to rigid body motion have been considered. Full scale hypersonic airbreathing vehicles are expected to be long and slender and thus highly flexible. This structural bending affects downstream flow resulting in localized changes in surface pressure along the body and thus, should be incorporated into the model. In this section, the flexible effects are included in the analysis. Piston theory is still used to determine the pressure distribution on the surfaces of the vehicle and much of the analysis already presented can be easily adapted to included these additional effects.

### A. Flexible Model

In order to develop the aeroelastic model, a few assumptions are made. First, the flexible vehicle is modelled as two cantilever beams fixed at the c.g. (one for the forebody section of the vehicle and one for the aftbody section of the vehicle). Second, the beams are assumed to have constant mass density, area, and flexural rigidity (EI), where EI is chosen to give the desired natural frequency of vibration. Also, it is assumed that the flexible effects only perturb the surface velocities in the z (normal) direction. This assumption is justified using the small angle approximation, i.e., the deflection of the tip of the beam is small compared to the length of the beam. Lastly, it is assumed that the change in angle of attack, as seen by the entire forebody, is the change in angle of attack as seen by the tip of the vehicle, point  $(\bar{x}_f, 0)$  in Fig. 1. Since the tip experiences the largest deflection, this is a worst-case assumption. This change in angle of attack is used to compute the flow properties behind the bow shock and those flow properties are assumed constant over the lower forebody.

The transverse vibrations in the beam satisfy the following partial differential equation:<sup>8</sup>

$$EI \frac{\partial^4 w(x, t)}{\partial x^4} + \hat{m} \frac{\partial^2 w(x, t)}{\partial t^2} = 0 \quad (50)$$

where  $w(x, t)$  describes the position of the beam, relative to the body x-axis,  $E$  is Young's Modulus,  $I$  is the moment of inertia of the beam cross-section about the y-axis, and  $\hat{m}$  is the mass density of the beam. This problem is typically solved using separation of variables. Assume

$$w(x, t) = \Phi(x)\eta(t) \quad (51)$$

Substituting the expression for  $w(x, t)$  in Eq. 51 into Eq. 50 and simplifying yields

$$\frac{EI}{\hat{m}\Phi(x)} \frac{\partial^4 \Phi(x)}{\partial x^4} = -\frac{1}{\eta(t)} \frac{\partial^2 \eta(t)}{\partial t^2} \quad (52)$$

Since the left side of Eq. 52 does not change as time varies, the right side of Eq. 52 must be a constant. Similarly, since the right side of Eq. 52 does not change as  $x$  varies, the left side of Eq. 52 must be a constant. Let this constant be  $\omega^2$ , such that

$$\frac{EI}{\hat{m}\Phi(x)} \frac{\partial^4 \Phi(x)}{\partial x^4} = -\frac{1}{\eta(t)} \frac{\partial^2 \eta(t)}{\partial t^2} = \omega^2 \quad (53)$$

Utilizing the method of separation of variables, Eq. 53 can be written as two differential equations, one with respect to position and one with respect to time:

$$\frac{\partial^4 \Phi(x)}{\partial x^4} - \beta^4 \Phi(x) = 0 \quad (54)$$

$$\frac{\partial^2 \eta(t)}{\partial t^2} + \omega^2 \eta(t) = 0 \quad (55)$$

where  $\beta^4 = \frac{\omega^2 \hat{m}}{EI}$ . The general solution to Eq. 54 is<sup>8</sup>

$$\Phi(x) = C_1 \sin \beta x + C_2 \cos \beta x + C_3 \sinh \beta x + C_4 \cosh \beta x \quad (56)$$

Using the following boundary conditions for the forward beam

$$\begin{aligned} \frac{d^2 \Phi(x)}{dx^2} \Big|_{x=\bar{x}_f} &= 0 & \frac{d^3 \Phi(x)}{dx^3} \Big|_{x=\bar{x}_f} &= 0 \\ \Phi(x) \Big|_{x=0} &= 0 & \frac{d\Phi(x)}{dx} \Big|_{x=0} &= 0 \end{aligned} \quad (57)$$

which state that the bending moment and shear force are zero at the free location ( $x = \bar{x}_f$ ) and the displacement and slope are zero at the fixed location ( $x = 0$ ), along with the modal shape expression, (Eq. 56), and simplifying results in the frequency equation

$$\cos \beta_f \bar{x}_f \cosh \beta_f \bar{x}_f = -1 \quad (58)$$

Eq. 58 has an infinite number of solutions with the first few given by

$$\beta_{f,r} \bar{x}_f = 1.8751, 4.6941, 7.8548, 10.9955, 14.1372, \dots \quad (59)$$

The values of  $\beta_{f,r}$ ,  $r = 1, 2, 3, \dots$  in Eq. 59 are called the eigenvalues. Corresponding to these eigenvalues, the natural modes of the forward beam are<sup>8</sup>

$$\begin{aligned} \Phi_{f,r}(x) = A_{f,r} [ & (\sin \beta_{f,r} \bar{x}_f - \sinh \beta_{f,r} \bar{x}_f) (\sin \beta_{f,r} x - \sinh \beta_{f,r} x)] \\ & + A_{f,r} [(\cos \beta_{f,r} \bar{x}_f + \cosh \beta_{f,r} \bar{x}_f) (\cos \beta_{f,r} x - \cosh \beta_{f,r} x)] \end{aligned} \quad (60)$$

where  $A_{f,r}$  is a normalizing factor, selected such that

$$\int_0^{\bar{x}_f} \hat{m}_f \Phi_{f,r}^2(x) dx = 1 \quad (61)$$

where  $\hat{m}_f$  is the mass density of the forebody beam defined as

$$\hat{m}_f = \frac{Mass \left(1 - \frac{\bar{x}_f}{L}\right)}{\bar{x}_f} \quad (62)$$

Thus,  $A_{f,r}$  becomes

$$A_{f,r} = \frac{1}{\sqrt{\hat{m}_f \left[ A_{f,r_{P_1}} + A_{f,r_{P_2}} + A_{f,r_{P_3}} \right]}} \quad (63)$$

where

$$A_{f,r_{P_1}} = \frac{(\sin \beta_{f,r} \bar{x}_f - \sinh \beta_{f,r} \bar{x}_f)^2}{4\beta_{f,r}} [M_{1f}] \quad (64)$$

$$A_{f,r_{P_2}} = \frac{(\sin \beta_{f,r} \bar{x}_f - \sinh \beta_{f,r} \bar{x}_f) (\cos \beta_{f,r} \bar{x}_f + \cosh \beta_{f,r} \bar{x}_f)}{\beta_{f,r}} (\sin \beta_{f,r} \bar{x}_f - \sinh \beta_{f,r} \bar{x}_f)^2 \quad (65)$$

$$A_{f,r_{P_3}} = \frac{(\cos \beta_{f,r} \bar{x}_f + \cosh \beta_{f,r} \bar{x}_f)^2}{4\beta_{f,r}} [M_{3f}] \quad (66)$$

and

$$M_{1f} = -2 \cos \beta_{f,r} \bar{x}_k \sin \beta_{f,r} \bar{x}_k + \sinh 2\beta_{f,r} \bar{x}_k - 4 \sin \beta_{f,r} \bar{x}_k \cosh \beta_{f,r} \bar{x}_k + 4 \cos \beta_{f,r} \bar{x}_k \sinh \beta_{f,r} \bar{x}_k \quad (67)$$

$$M_{3f} = 2 \cos \beta_{f,r} \bar{x}_k \sin \beta_{f,r} \bar{x}_k + \sinh 2\beta_{f,r} \bar{x}_k - 4 \cos \beta_{f,r} \bar{x}_k \sinh \beta_{f,r} \bar{x}_k - 4 \sin \beta_{f,r} \bar{x}_k \cosh \beta_{f,r} \bar{x}_k + 4\beta_{f,r} \bar{x}_k \quad (68)$$

For the aft beam, the boundary conditions are

$$\begin{aligned} \frac{d^2 \Phi(x)}{dx^2} \Big|_{x=\bar{x}_a} = 0 & \quad \frac{d^3 \Phi(x)}{dx^3} \Big|_{x=\bar{x}_a} = 0 \\ \Phi(x) \Big|_{x=0} = 0 & \quad \frac{d\Phi(x)}{dx} \Big|_{x=0} = 0 \end{aligned} \quad (69)$$

and the frequency equation becomes

$$\cos \beta_a \bar{x}_a \cosh \beta_a \bar{x}_a = -1 \quad (70)$$

with solutions

$$\beta_{a,r} \bar{x}_a = 1.8751, 4.6941, 7.8548, 10.9955, 14.1372, \dots \quad (71)$$

The natural modes of the aft beam are

$$\begin{aligned} \Phi_{a,r}(x) = A_{a,r} [ & (\sin \beta_{a,r} \bar{x}_a - \sinh \beta_{a,r} \bar{x}_a) (\sin \beta_{a,r} x - \sinh \beta_{a,r} x)] \\ & + A_{a,r} [(\cos \beta_{a,r} \bar{x}_a + \cosh \beta_{a,r} \bar{x}_a) (\cos \beta_{a,r} x - \cosh \beta_{a,r} x)] \end{aligned} \quad (72)$$

and  $A_{a,r}$  is selected such that

$$\int_0^{\bar{x}_a} \hat{m}_a \Phi_{a,r}^2(x) dx = 1 \quad (73)$$

and

$$\hat{m}_a = \frac{Mass \left(1 - \frac{\bar{x}_a}{L}\right)}{\bar{x}_a} \quad (74)$$

Thus,  $A_{a,r}$  becomes

$$A_{a,r} = \frac{1}{\sqrt{\hat{m}_a \left[ A_{a,r_{P_1}} + A_{a,r_{P_2}} + A_{a,r_{P_3}} \right]}} \quad (75)$$

where

$$A_{a,r_{P_1}} = \frac{(\sin \beta_{a,r} \bar{x}_a - \sinh \beta_{a,r} \bar{a}_f)^2}{4\beta_{a,r}} [M_{1a}] \quad (76)$$

$$A_{a,r_{P_2}} = \frac{(\sin \beta_{a,r} \bar{x}_a - \sinh \beta_{a,r} \bar{x}_a) (\cos \beta_{a,r} \bar{x}_a + \cosh \beta_{a,r} \bar{x}_a)}{\beta_{a,r}} (\sin \beta_{a,r} \bar{x}_a - \sinh \beta_{a,r} \bar{x}_a)^2 \quad (77)$$

$$A_{a,r_{P_3}} = \frac{(\cos \beta_{a,r} \bar{x}_a + \cosh \beta_{a,r} \bar{x}_a)^2}{4\beta_{a,r}} [M_{3a}] \quad (78)$$

and

$$M_{1a} = -2 \cos \beta_{a,r} \bar{x}_a \sin \beta_{a,r} \bar{x}_a + \sinh 2\beta_{a,r} \bar{x}_a - 4 \sin \beta_{a,r} \bar{x}_a \cosh \beta_{a,r} \bar{x}_a + 4 \cos \beta_{a,r} \bar{x}_a \sinh \beta_{a,r} \bar{x}_a \quad (79)$$

$$M_{3a} = 2 \cos \beta_{a,r} \bar{x}_a \sin \beta_{a,r} \bar{x}_a + \sinh 2\beta_{a,r} \bar{x}_a - 4 \cos \beta_{a,r} \bar{x}_a \sinh \beta_{a,r} \bar{x}_a - 4 \sin \beta_{a,r} \bar{x}_a \cosh \beta_{a,r} \bar{x}_a + 4\beta_{a,r} \bar{x}_a \quad (80)$$

## B. Forced Response

Let the forcing function in Eq. 50 consist of distributed and concentrated loads so that Eq. 50 can be written as

$$EI \frac{\partial^4 w(x,t)}{\partial x^4} + \hat{m} \frac{\partial^2 w(x,t)}{\partial t^2} = f(x,t) + F_j(t) \delta(x - x_j) \quad (81)$$

where  $\delta(x)$  is the dirac delta function defined as

$$\delta(x - x_j) = \begin{cases} 1 & \text{if } x = x_j \\ 0 & \text{if } x \neq x_j \end{cases} \quad (82)$$

From the expansion theorem, the solution to Eq. 81 is

$$w_f(x,t) = \sum_{r=1}^{\infty} \Phi_{f,r}(x) \eta_{f,r}(t) \quad (83)$$

for the forebody beam and

$$w_a(x,t) = \sum_{r=1}^{\infty} \Phi_{a,r}(x) \eta_{a,r}(t) \quad (84)$$

for the aftbody beam where  $\eta_{f,r}(t)$ ,  $\eta_{a,r}(t)$  are the generalized modal coordinates, for the forebody and aftbody beams, that satisfy

$$\begin{aligned} \ddot{\eta}_{f,r}(t) + 2\zeta_{f,r} \omega_{f,r} \dot{\eta}_{f,r}(t) + \omega_{f,r}^2 \eta_{f,r}(t) &= N_{f,r}(t) \\ \ddot{\eta}_{a,r}(t) + 2\zeta_{a,r} \omega_{a,r} \dot{\eta}_{a,r}(t) + \omega_{a,r}^2 \eta_{a,r}(t) &= N_{a,r}(t) \end{aligned} \quad (85)$$

Here,  $N_{f,r}(t)$ ,  $N_{a,r}(t)$  are generalized forces for the  $r^{\text{th}}$  mode shape of the forebody/aftbody beam, defined by<sup>8</sup>

$$\begin{aligned} N_{f,r}(t) &= \int_0^{\bar{x}_f} \Phi_{f,r}(x) f_f(x,t) dx + \sum_{j=1}^n \Phi_{f,r}(x_j) F_{f,j}(t) \\ N_{a,r}(t) &= \int_0^{\bar{x}_a} \Phi_{a,r}(x) f_a(x,t) dx + \sum_{j=1}^n \Phi_{a,r}(x_j) F_{a,j}(t) \end{aligned} \quad (86)$$

where  $n$  is the number of concentrated loads on the beam. Given the loading on the forebody and aftbody beams, the generalized forces for the first mode become

$$\begin{aligned} N_{f,1}(t) &= \int_0^{\bar{x}_f} \Phi_{f,1}(x) P_{cf} dx - \int_{\bar{x}_f - L_f}^{\bar{x}_f} \Phi_{f,1}(x) P_{cd} dx + \Phi_{f,1}(x_{canard}) (P_{cU} - P_{cL}) L_c \\ N_{a,1}(t) &= \int_0^{\bar{x}_a} \Phi_{a,1}(x) P_{cf} dx - \int_{\bar{x}_a - L_a}^{\bar{x}_a} \Phi_{a,1}(x) P_{ef} dx + \Phi_{a,1}(x_{elev}) (P_{eU} - P_{eL}) L_e \end{aligned} \quad (87)$$

These expressions are displayed in Appendix A.

In order to incorporate aeroelastic effects into the model, a few simplifying assumptions are made. First, the vehicle does not stretch or compress along the  $x$ -axis. Second, for small displacements, when the beams (vehicle) flexes, there is no change in the  $x$  direction displacement. With these assumptions, aeroelastic effects only occur in the  $z$ -direction. Additionally, it is assumed that the engine nacelle is rigid. The aeroelastic effects can be accounted for by taking the time derivative of Eqs. 83 and 84

$$\begin{aligned} \dot{w}_f(x, t) &= \sum_{r=1}^{\infty} \Phi_{f,r}(x) \dot{\eta}_{f,r}(t) \\ \dot{w}_a(x, t) &= \sum_{r=1}^{\infty} \Phi_{a,r}(x) \dot{\eta}_{a,r}(t) \end{aligned} \quad (88)$$

and including this effect in the expressions for the velocities on the upper and lower surfaces, namely Eqs. 11, 12, and 14. The differential forces on the surfaces become

$$d\mathbf{F}_{cf_f} = (-P_{cf} - \rho_{cf} a_{cf} \{ [u + q \tan \tau_{1,U} (x - \bar{x}_f)] \sin \tau_{1,U} - [w - qx + \dot{w}_f(x, t)] \cos \tau_{1,U} \}) \sec \tau_{1,U} \mathbf{n}_{cf} dx \quad (89)$$

$$d\mathbf{F}_{cf_a} = (-P_{cf} - \rho_{cf} a_{cf} \{ [u + q \tan \tau_{1,U} (x - \bar{x}_f)] \sin \tau_{1,U} - [w - qx + \dot{w}_a(x, t)] \cos \tau_{1,U} \}) \sec \tau_{1,U} \mathbf{n}_{cf} dx \quad (90)$$

$$d\mathbf{F}_{cd} = (-P_{cd} - \rho_{cd} a_{cd} \{ [u - q \tan \tau_{1,L} (x - \bar{x}_f)] \sin \tau_{1,L} + [w - qx + \dot{w}_f(x, t)] \cos \tau_{1,L} \}) \sec \tau_{1,L} \mathbf{n}_{cd} dx \quad (91)$$

$$d\mathbf{F}_{ef} = (-P_{ef} - \rho_{ef} a_{ef} \{ -(u + q r_{efz}) \sin(\tau_{1,U} + \tau_2) + (w - qx + \dot{w}_a(x, t)) \cos(\tau_{1,U} + \tau_2) \}) \sec(\tau_{1,U} + \tau_2) \mathbf{n}_{ef} dx \quad (92)$$

where the upper surface force has been split into forebody and aftbody parts to account for the two beam structural model. With these differential forces, stability derivatives due to the bending of the vehicle can be determined. For the normal force on the forebody beam,

$$\begin{aligned} (C_Z)_{\dot{w}_{forebody}} &= \frac{1}{q_{\infty} S} \left[ \int_0^{\bar{x}_f} (d\mathbf{F}_{cf})_{z-\dot{w}} + \int_{\bar{x}_f - L_f}^{\bar{x}_f} (d\mathbf{F}_{cd})_{z-\dot{w}} \right] \\ &= \frac{1}{q_{\infty} S} \int_0^{\bar{x}_f} -\rho_{cf} a_{cf} \dot{w} \cos \tau_{1,U} dx + \int_{\bar{x}_f - L_f}^{\bar{x}_f} -\rho_{cd} a_{cd} \dot{w} \cos \tau_{1,L} dx \end{aligned} \quad (93)$$

Substituting Eq. 88 into Eq. 93 produces

$$(C_Z)_{\dot{w}_{forebody}} = \frac{1}{q_{\infty} S} \int_0^{\bar{x}_f} -\rho_{cf} a_{cf} \sum_{r=1}^{\infty} \Phi_{f,r}(x) \dot{\eta}_{f,r}(t) \cos \tau_{1,U} dx + \int_{\bar{x}_f - L_f}^{\bar{x}_f} -\rho_{cd} a_{cd} \sum_{r=1}^{\infty} \Phi_{f,r}(x) \dot{\eta}_{f,r}(t) \cos \tau_{1,L} dx \quad (94)$$

which, for the first bending mode becomes

$$\begin{aligned} \frac{\partial C_Z}{\partial \dot{\eta}_{f,1}} &= \frac{1}{q_{\infty} S} \int_0^{\bar{x}_f} -\rho_{cf} a_{cf} \Phi_{f,1}(x) \cos \tau_{1,U} dx + \int_{\bar{x}_f - L_f}^{\bar{x}_f} -\rho_{cd} a_{cd} \Phi_{f,1}(x) \cos \tau_{1,L} dx \\ &= \frac{1}{q_{\infty} S} \left[ \frac{-2\rho_{cf} a_{cf} \cos \tau_{1,U} A_{f,1}}{\beta_{f,1}} (\sin \beta_{f,1} \bar{x}_f - \sinh \beta_{f,1} \bar{x}_f) \right] \\ &\quad - \frac{\rho_{cd} a_{cd} \cos \tau_{1,L} A_{f,1}}{\beta_{f,1} q_{\infty} S} [(\sin \beta_{f,1} \bar{x}_f - \sinh \beta_{f,1} \bar{x}_f) (\cos \beta_{f,1} (\bar{x}_f - L_f) + \cosh \beta_{f,1} (\bar{x}_f - L_f))] \\ &\quad - \frac{\rho_{cd} a_{cd} \cos \tau_{1,L} A_{f,1}}{\beta_{f,1} q_{\infty} S} [(\cos \beta_{f,1} \bar{x}_f + \cosh \beta_{f,1} \bar{x}_f) (-\sin \beta_{f,1} (\bar{x}_f - L_f) + \sinh \beta_{f,1} (\bar{x}_f - L_f))] \end{aligned} \quad (95)$$

where  $A_{f,1}$  is the normalizing factor associated with the first mode. Using the assumption that the flexible effects only perturb the surface velocities in the z-direction, the axial force stability derivative associated with the flexible effect becomes

$$\frac{\partial C_X}{\partial \dot{\eta}_{f,1 \text{ forebody}}} = 0 \quad (96)$$

For the pitching moment,

$$(C_M)_{\dot{w}_{f \text{ forebody}}} = \frac{1}{q_\infty S \bar{c}} \left[ \int_0^{\bar{x}_f} z (d\mathbf{F}_{cf})_{x-\dot{w}} + \int_{\bar{x}_f-L_f}^{\bar{x}_f} z (d\mathbf{F}_{cd})_{x-\dot{w}} \right] - \frac{1}{q_\infty S \bar{c}} \left[ \int_0^{\bar{x}_f} x (d\mathbf{F}_{cf})_{z-\dot{w}} + \int_{\bar{x}_f-L_f}^{\bar{x}_f} x (d\mathbf{F}_{cd})_{z-\dot{w}} \right] \quad (97)$$

For the first mode only, this expression is displayed in Appendix A.

For the aftbody beam, the Z direction force due to flexibility is

$$(C_Z)_{\dot{w}_{a \text{ aftbody}}} = \frac{1}{q_\infty S} \left[ \int_0^{\bar{x}_a} (d\mathbf{F}_{cf})_{z-\dot{w}} + \int_{\bar{x}_a-L_a}^{\bar{x}_a} (d\mathbf{F}_{ef})_{z-\dot{w}} \right] \quad (98)$$

and this expression is evaluated in Appendix A.

The pitching moment coefficient due to aftbody flexibility is

$$(C_M)_{\dot{w}_{a \text{ aftbody}}} = \frac{1}{q_\infty S \bar{c}} \left[ \int_0^{\bar{x}_a} z (d\mathbf{F}_{cf})_{x-\dot{w}} + \int_{\bar{x}_a-L_a}^{\bar{x}_a} z (d\mathbf{F}_{ef})_{x-\dot{w}} \right] - \frac{1}{q_\infty S \bar{c}} \left[ \int_0^{\bar{x}_a} x (d\mathbf{F}_{cf})_{z-\dot{w}} + \int_{\bar{x}_a-L_a}^{\bar{x}_a} x (d\mathbf{F}_{ef})_{z-\dot{w}} \right] \quad (99)$$

and this expression is evaluated in Appendix A for the first bending mode.

With the inclusion of the flexible stability derivatives, the total aerodynamic forces and moments on the vehicle are

$$X_{total} = X_{cf_f} + X_{cf_a} + X_{cd} + X_{gh} + X_{ef} + X_{e_L} + X_{e_U} + X_{c_U} + X_{c_L} + T + q_\infty S \frac{\partial C_X}{\partial \alpha} \alpha + q_\infty S \left( \frac{\partial C_X}{\partial \alpha} \right)_{\delta_e} \alpha + q_\infty S \left( \frac{\partial C_X}{\partial \alpha} \right)_{\delta_c} \alpha \quad (100)$$

$$Z_{total} = Z_{cf_f} + Z_{cf_a} + Z_{cd} + Z_{gh} + Z_{ef} + Z_{e_L} + Z_{e_U} + Z_{c_U} + Z_{c_L} + q_\infty S \frac{\partial C_Z}{\partial \alpha} \alpha + q_\infty S \frac{\partial C_Z}{\partial q} \frac{q\bar{c}}{2V_\infty} + q_\infty S \left( \frac{\partial C_Z}{\partial \alpha} \right)_{\delta_e} \alpha + q_\infty S \left( \frac{\partial C_Z}{\partial \alpha} \right)_{\delta_c} \alpha + q_\infty S \left( \frac{\partial C_Z}{\partial q} \right)_{\delta_e} \frac{q\bar{c}}{2V_\infty} + q_\infty S \left( \frac{\partial C_Z}{\partial q} \right)_{\delta_c} \frac{q\bar{c}}{2V_\infty} + q_\infty S \frac{\partial C_Z}{\partial \dot{\eta}_{a,1}} + q_\infty S \frac{\partial C_Z}{\partial \dot{\eta}_{f,1}} \quad (101)$$

$$M_{total} = M_{cf_f} + M_{cf_a} + M_{cd} + M_{gh} + M_{ef} + M_{e_L} + M_{e_U} + M_{c_U} + M_{c_L} + M_{engine} + q_\infty S \bar{c} \frac{\partial C_M}{\partial \alpha} \alpha + q_\infty S \bar{c} \frac{\partial C_M}{\partial q} \frac{q\bar{c}}{2V_\infty} + q_\infty S \bar{c} \left( \frac{\partial C_M}{\partial \alpha} \right)_{\delta_e} \alpha + q_\infty S \bar{c} \left( \frac{\partial C_M}{\partial \alpha} \right)_{\delta_c} \alpha + q_\infty S \bar{c} \left( \frac{\partial C_M}{\partial q} \right)_{\delta_e} \frac{q\bar{c}}{2V_\infty} + q_\infty S \bar{c} \left( \frac{\partial C_M}{\partial q} \right)_{\delta_c} \frac{q\bar{c}}{2V_\infty} + q_\infty S \bar{c} \frac{\partial C_M}{\partial \dot{\eta}_{a,1}} \dot{\eta}_{a,1} + q_\infty S \bar{c} \frac{\partial C_M}{\partial \dot{\eta}_{f,1}} \dot{\eta}_{f,1} \quad (102)$$

### C. Equations of Motion for a Flexible Vehicle

The equations of motion for the flexible vehicle are<sup>6</sup>

$$\begin{aligned}
\dot{V}_T &= \frac{1}{m} (T \cos \alpha - D) - g \sin(\theta - \alpha) \\
\dot{\alpha} &= \frac{1}{mV_T} (-T \sin \alpha - L) + Q + \frac{g}{V_T} \cos(\theta - \alpha) \\
I_{yy} \dot{Q} - \Psi_f \ddot{\eta}_f - \Psi_a \ddot{\eta}_a &= M \\
\dot{\theta} &= Q \\
k_f \ddot{\eta}_f + 2\zeta_f \omega_f \dot{\eta}_f + \omega_f^2 \eta_f &= N_f - \Psi_f \frac{M}{I_{yy}} - \frac{\Psi_f \Psi_a \ddot{\eta}_a}{J_{yy}} \\
k_a \ddot{\eta}_a + 2\zeta_a \omega_a \dot{\eta}_a + \omega_a^2 \eta_a &= N_a - \Psi_a \frac{M}{I_{yy}} - \frac{\Psi_f \Psi_a \ddot{\eta}_f}{J_{yy}} \\
\dot{h} &= V_T \sin(\theta - \alpha)
\end{aligned} \tag{103}$$

where

$$\begin{aligned}
\Psi_f &= \int_0^{\bar{x}_f} x \Phi_{f,1}(x) dx \\
k_f &= 1 + \frac{\Psi_f}{I_{yy}} \\
\Psi_a &= \int_0^{\bar{x}_a} x \Phi_{a,1}(x) dx \\
k_a &= 1 + \frac{\Psi_a}{I_{yy}}
\end{aligned} \tag{104}$$

Clearly, the flexible effects are coupled into the pitch rate equation. In addition to this, the bending of the structure has an effect on the angle of attack of the vehicle. Since engine performance is a function of shock angle and shock angle is a function of angle of attack, a significant change to the vehicle's performance can occur due to structural bending. It is assumed, from the point of view of the bow shock, that the entire forebody observes the same change in angle of attack as seen at the nose of the vehicle. In other words, the worst case change in angle of attack is used for the entire forebody. This change in angle of attack is computed as:

$$\Delta\alpha = \arctan [\Phi'_f(\bar{x}_f) \eta_{f,1}(t)] \tag{105}$$

The control surfaces also see a change in angle of attack, which affects the properties of the flow over the surfaces. These changes are given by

$$\Delta\alpha_{canard} = \arctan [\Phi'_f(x_{canard}) \eta_{f,1}(t)] \tag{106}$$

$$\Delta\alpha_{cs} = \arctan [\Phi'_a(x_{elev}) \eta_{a,1}(t)] \tag{107}$$

so that the total angle of attack seen by the control surfaces is

$$\begin{aligned}
\alpha_{canard} &= \alpha + \Delta\alpha_{canard} \\
\alpha_{elev} &= \alpha + \Delta\alpha_{elev}
\end{aligned} \tag{108}$$

The forces due to the control effectors, as given in Eqs. 20, 21 and 30 are written in the rigid vehicle's body axis frame. However, when the structure bends, these forces are not aligned with the body axis and therefore, must be rotated back into the body axis frame. This is accomplished using

$$\begin{aligned}
\mathbf{F}_{eV} &= P_{eV} L_e \sin(\delta_e + \Delta\alpha_e) \hat{i} + P_{eV} L_e \cos(\delta_e + \Delta\alpha_e) \hat{k} \\
\mathbf{F}_{eL} &= -P_{eL} L_e \sin(\delta_e + \Delta\alpha_e) \hat{i} - P_{eL} L_e \cos(\delta_e + \Delta\alpha_e) \hat{k}
\end{aligned} \tag{109}$$

and

$$\begin{aligned}
\mathbf{F}_{cV} &= P_{cV} L_c \sin(\delta_c + \Delta\alpha_c) \hat{i} + P_{cV} L_c \cos(\delta_c + \Delta\alpha_c) \hat{k} \\
\mathbf{F}_{cL} &= -P_{cL} L_c \sin(\delta_c + \Delta\alpha_c) \hat{i} - P_{cL} L_c \cos(\delta_c + \Delta\alpha_c) \hat{k}
\end{aligned} \tag{110}$$

In terms of the calculation of the moments produced by the controls, the moment arm is also altered by the flexible effects. For small displacements of the beams relative to their lengths, the new moment arms become

$$\begin{aligned}
\mathbf{r}_{canard} &= \left( \sqrt{x_{canard}^2 - (\Phi_f(x_{canard}) \eta_{f,1})^2}, \Phi_f(x_{canard}) \eta_{f,1} \right) \\
\mathbf{r}_{elev} &= \left( \sqrt{x_{elev}^2 + z_{elev}^2 - (z_e + \Phi_a(x_{elev}) \eta_{a,1})^2}, z_{elev} + \Phi_a(x_{elev}) \eta_{a,1} \right)
\end{aligned} \tag{111}$$

## VIII. Results

The model has been linearized at  $M = 8$  and at an altitude of 85,000 ft using velocity and flight path angle as outputs and elevator deflection and total temperature addition in the combustor as inputs. One point of interest that can be obtained from this simulation is the effect of the unsteady terms on the poles and zeros of the linearized system. Figure 2 shows a pole/zero map for the linearized rigid body system when unsteady effects are not included, while Fig. 3 shows the poles and zeros of the rigid body system when the unsteady effects are included. Clearly, the unsteady terms have a significant effect on the unstable pole and zero. Inclusion of the unsteady terms makes the system more unstable, while increasing the frequency of the non-minimum phase zero. The actual pole and zero locations are given in Table 1.

Unsteady OFF	Unsteady OFF	Unsteady ON	Unsteady ON
Poles	Zeros	Poles	Zeros
$-0.000137 \pm j0.023358$	1.8694	$-0.000151 \pm j0.02332$	2.64
0.8729	-1.8694	1.125	-2.64
-0.9159	0	-1.216	0
-.00107	N/A	-.001027	N/A

Table 1. Poles and Zeros of the Rigid Linearized System.

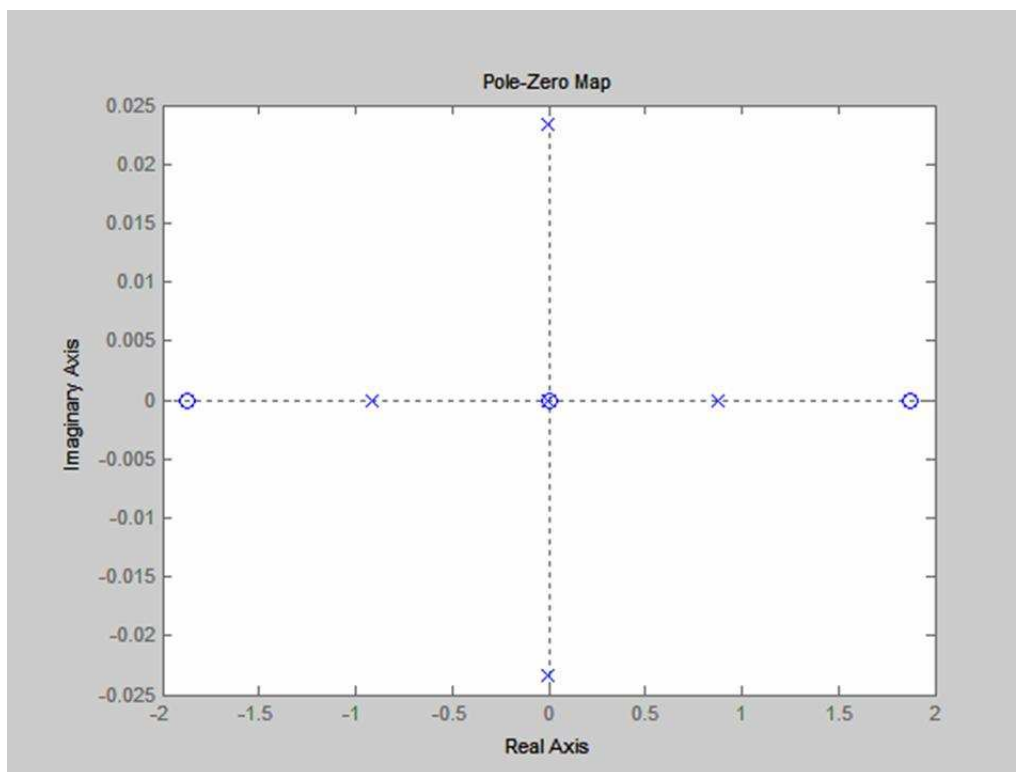


Figure 2. Poles and Zeros of Linearized Rigid Body System - Unsteady Effects Off.

Now, the flexible effects are included in the vehicle model. Figure 4 shows a pole/zero map for the flexible vehicle when unsteady effects are not included. Figures 5 and 6 show pole/zero maps when the unsteady effects are included. The difference here is that the stability derivatives due to  $\dot{\eta}_{f,1}$  and  $\dot{\eta}_{a,1}$  are included in Fig. 6 while they are not in the results shown in Fig. 5. In tabular form, the poles and zeros are shown in Table 2.

It can be seen that the unsteady effects, computed using piston theory, significantly change the poles and

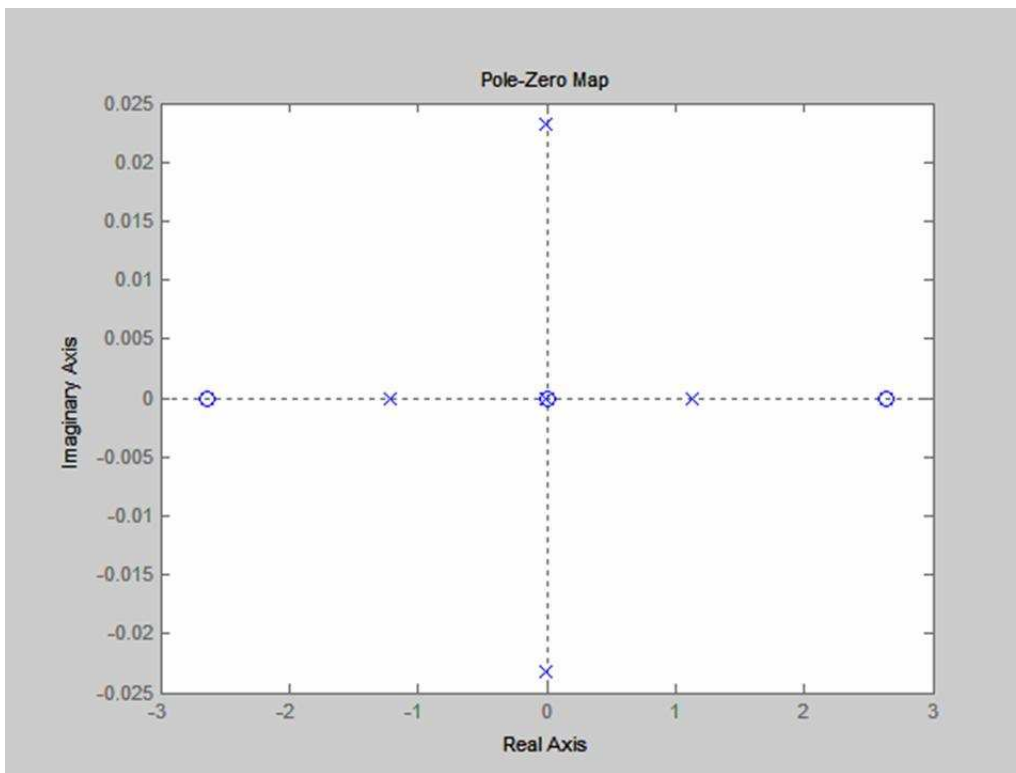


Figure 3. Poles and Zeros of Linearized Rigid Body System - Unsteady Effects On.

All Unsteady OFF	
Poles	Zeros
$-.538 \pm j26.909$	$-.538 \pm j26.904$
$-.36 \pm j17.99$	$-.36 \pm j17.99$
1.23	2.64
-1.32	-2.64
-.00088	0
$-.00012 \pm j.024$	N/A

Table 2. Poles and Zeros of the Flexible Linearized System With All Unsteady Effects Off.

Unsteady On & Unsteady Flex. OFF	
Poles	Zeros
$-.538 \pm j26.91$	$-.538 \pm j26.91$
$-.36 \pm j17.99$	$-.36 \pm j17.99$
1.88	3.88
-2.06	-3.88
-.00086	0
$-.00012 \pm j.024$	N/A

Table 3. Poles and Zeros of the Flexible Linearized System With Unsteady Effects On and Flexible Unsteady Effects Off.

Unsteady On & Unsteady Flex. ON	
Poles	Zeros
$-.55 \pm j26.91$	$-.56 \pm j26.89$
$-.36 \pm j17.99$	$-.36 \pm j17.99$
1.88	3.88
-2.06	-3.88
-.00086	0
$-.00012 \pm j.024$	N/A

Table 4. Poles and Zeros of the Flexible Linearized System With Unsteady Effects On and Flexible Unsteady Effects On.

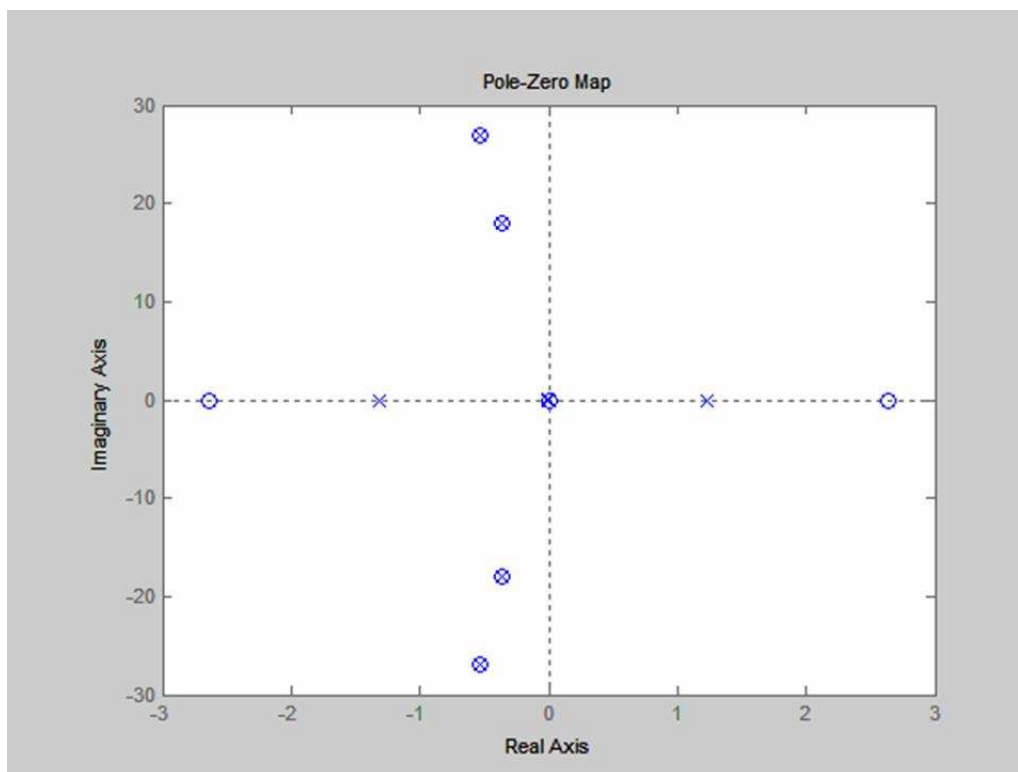


Figure 4. Poles and Zeros of Linearized Flexible System - Unsteady Effects Off.

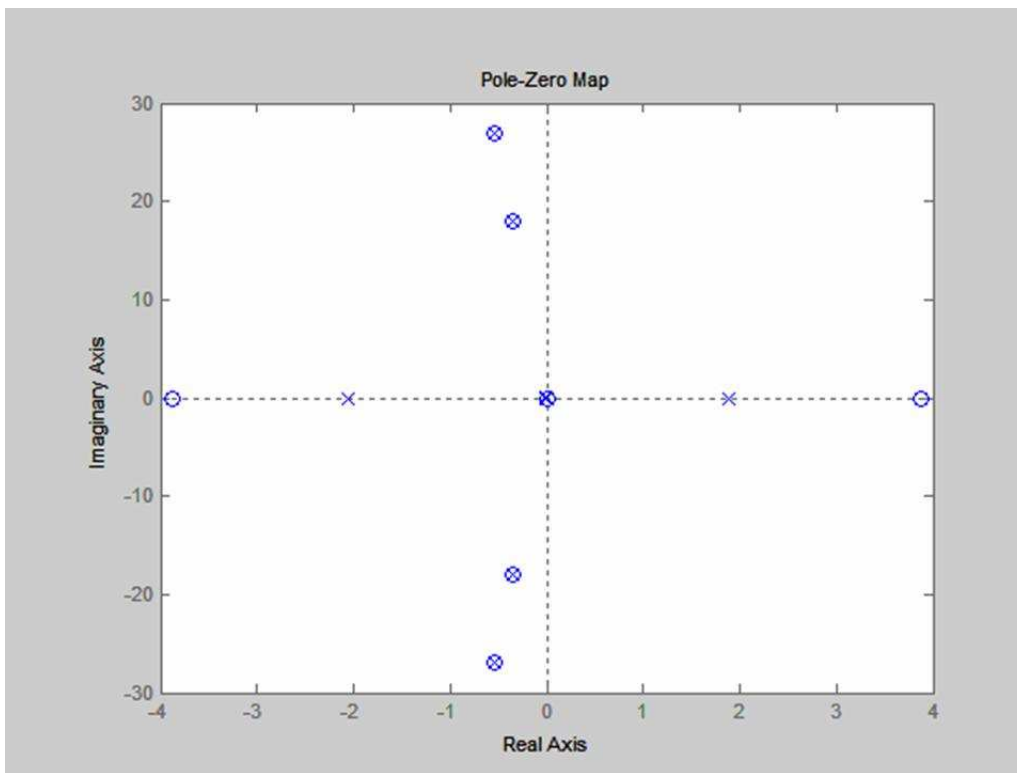


Figure 5. Poles and Zeros of Linearized Flexible System - Unsteady Effects On, Unsteady Flexible Effects Off.

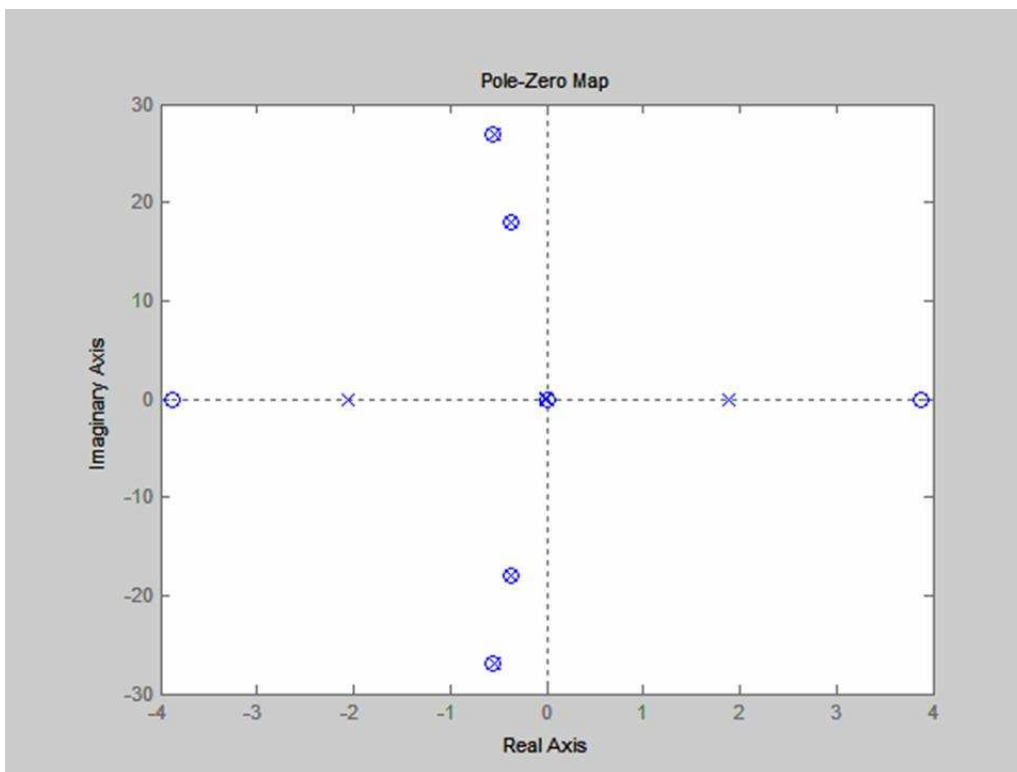


Figure 6. Poles and Zeros of Linearized Flexible System - Unsteady Effects On, Unsteady Flexible Effects On.

zeros of the linearized system. Both the unstable pole and zero of the linearized system move farther to the right in the s-plane when the unsteady effects are included. Only a slight change in pole and zero locations is observed when the unsteady effects due to  $\dot{\eta}$  are included.

Figures 7, 8, and 9 show the lift force, drag force, and pitching moment for a one second run of the nonlinear simulation. Again, it can be seen that the unsteady effects are significant and are worth including in the nonlinear simulation.

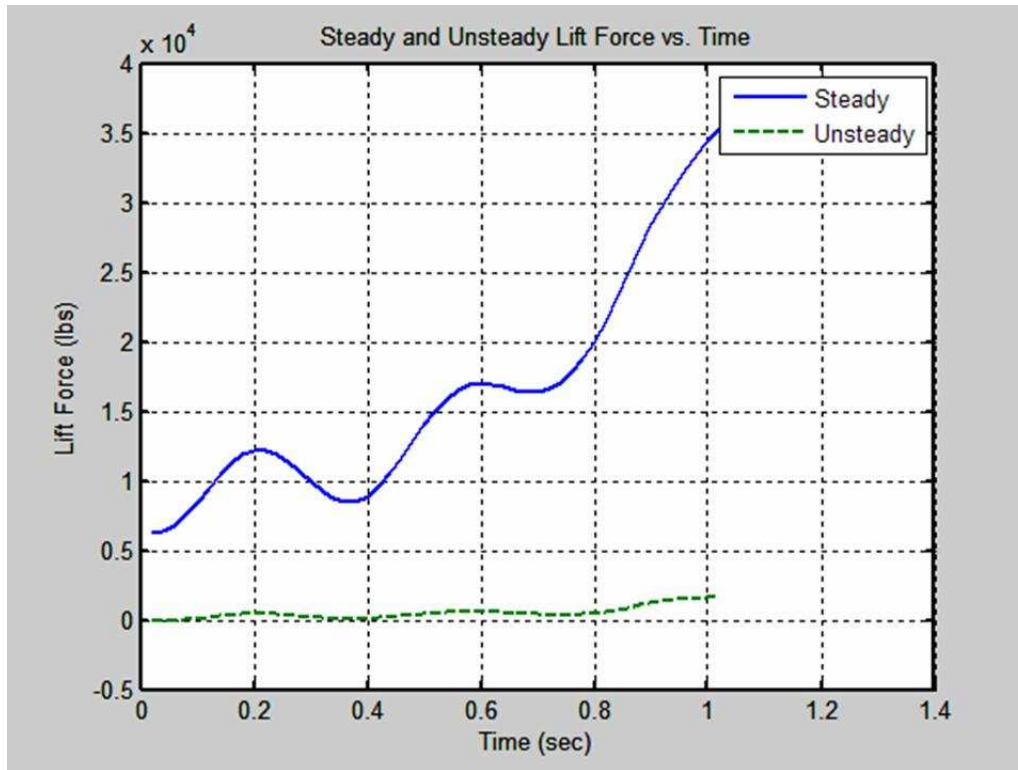


Figure 7. Lift Force (lbs).

## IX. Conclusions

In this work, piston theory is used to develop a model for the longitudinal dynamics of a 2-dimensional hypersonic vehicle model. In particular, velocities of flow normal to the surface of the vehicle are used in a first order piston theory framework to determine the pressures on the surfaces of the vehicle. The pressures are then integrated over the body to determine the forces acting on the vehicle. Piston theory is useful here because it allows the inclusion of unsteady aerodynamic effects. Initial analysis has shown that the unsteady effects are significant.

## References

- <sup>1</sup>Lighthill, M., "Oscillating Airfoils at High Mach Number," *Journal of the Aeronautical Sciences*, Vol. 20, No. 6, 1953, pp. 402–406.
- <sup>2</sup>Ashley, H. and Zartarian, G., "Piston Theory - A New Aerodynamic Tool for the Aeroelastician," *Journal of the Aeronautical Sciences*, 1956, pp. 1109–1118.
- <sup>3</sup>Tarpley, C. and Lewis, M., "Stability Derivatives for a Hypersonic Caret-Wing Waverider," *Journal of Aircraft*, Vol. 32, No. 4, 1995, pp. 795–803.
- <sup>4</sup>McNamara, J. and Friedmann, P., "Aeroelastic and Aerothermoelastic Analysis of Hypersonic Vehicles: Current Status and Future Trends," *48th AIAA/ASME/ASCE/AHS/ASC Structures, Structural Dynamics, and Materials Conference*, AIAA-2007-2013, April 2007.
- <sup>5</sup>Oppenheimer, M. W. and Doman, D. B., "A Hypersonic Vehicle Model Developed with Piston Theory," *Proceedings of*

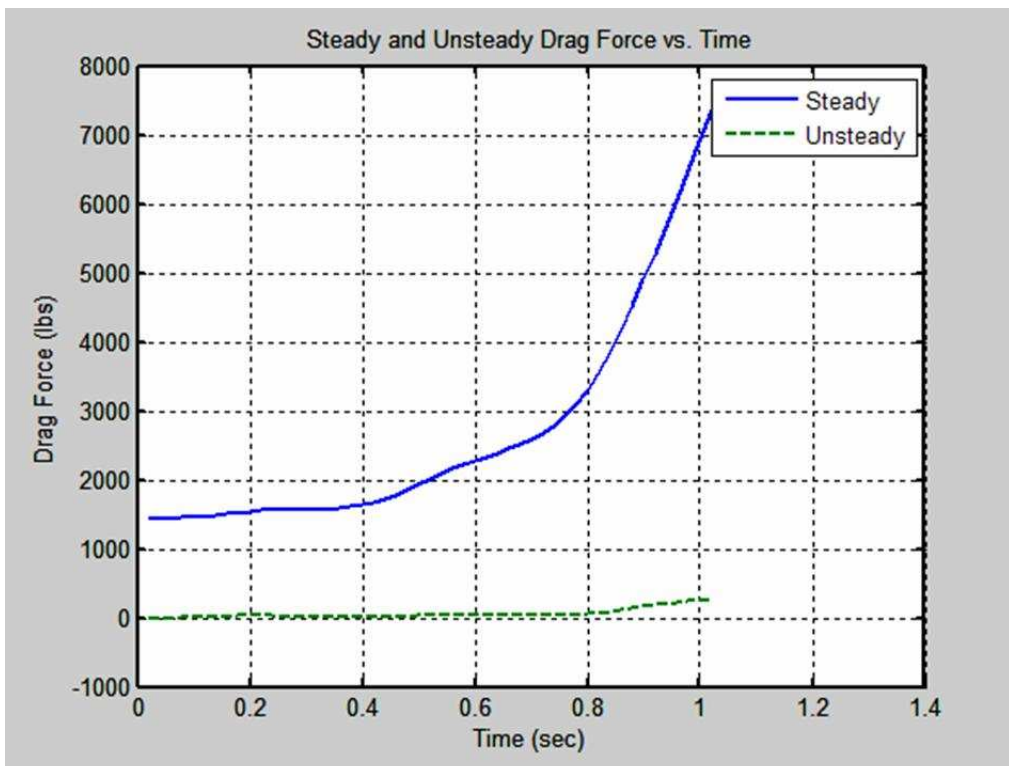


Figure 8. Drag Force (lbs).

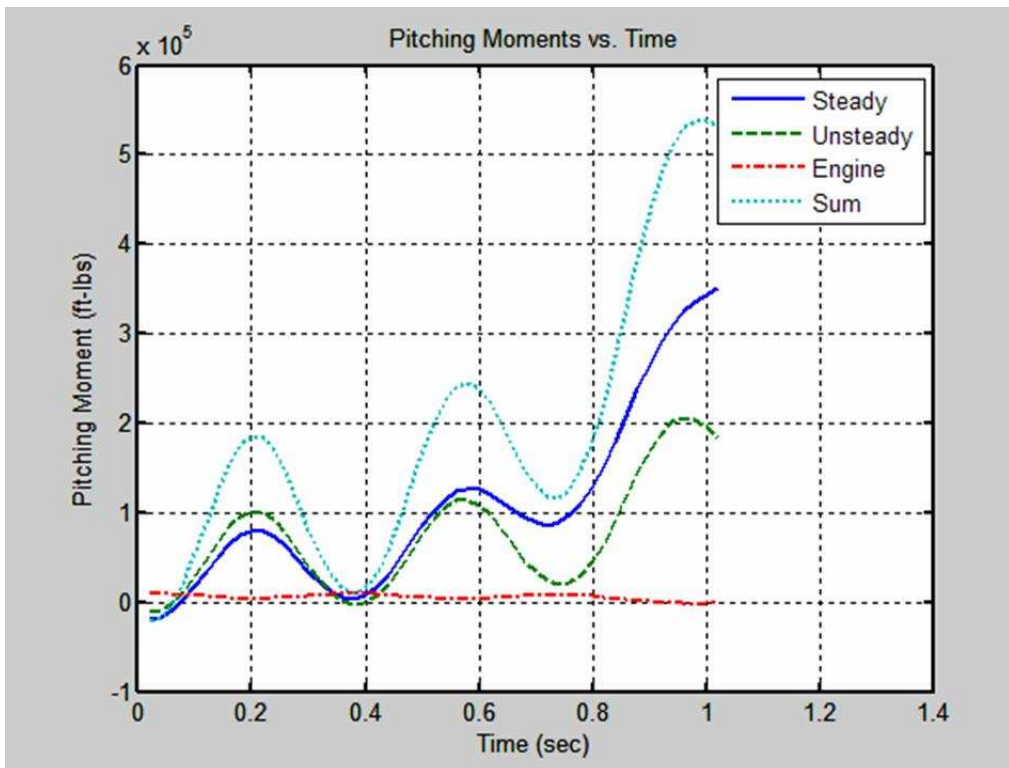


Figure 9. Pitching Moment (ft-lbs).

the 2006 AIAA Atmospheric Flight Mechanics Conference, AIAA-2006-6637, August 2006.

<sup>6</sup>Bolender, M. A. and Doman, D. B., "A Non-Linear Model for the Longitudinal Dynamics of a Hypersonic Airbreathing Vehicle," *Proceedings of the 2005 Guidance, Navigation and Control Conference*, AIAA Paper No. 2005-6255, August 2005.

<sup>7</sup>Bolender, M. A. and Doman, D. B., "Flight Path Angle Dynamics of Air-Breathing Hypersonic Vehicles," *Proceedings of the 2006 AIAA Guidance, Navigation, and Control Conference*, AIAA-2006-6692, August 2006.

<sup>8</sup>Meirovitch, L., *Analytical Methods in Vibrations*, The Macmillan Company, New York, NY, 1967.

## A. Flexible Effects

From Eq. 87

$$\begin{aligned}
N_{f,1}(t) &= \frac{A_{f,1}P_{cf}}{\beta_{f,1}} [(-\sin\{\beta_{f,1}\bar{x}_f\} + \sinh\{\beta_{f,1}\bar{x}_f\}) (\cos\{\beta_{f,1}\bar{x}_f\} + \cosh\{\beta_{f,1}\bar{x}_f\} - 2)] \\
&\quad + \frac{A_{f,1}P_{cf}}{\beta_{f,1}} [(\cos\{\beta_{f,1}\bar{x}_f\} + \cosh\{\beta_{f,1}\bar{x}_f\}) (\sin\{\beta_{f,1}\bar{x}_f\} - \sinh\{\beta_{f,1}\bar{x}_f\})] \\
&+ \frac{A_{f,1}P_{cd}}{\beta_{f,1}} [(-\sin\{\beta_{f,1}\bar{x}_f\} + \sinh\{\beta_{f,1}\bar{x}_f\}) (\cos\{\beta_{f,1}\bar{x}_f\} - \cos\{\beta_{f,1}(\bar{x}_f - L_f)\}) + \cosh\{\beta_{f,1}\bar{x}_f\} - \cosh\{\beta_{f,1}(\bar{x}_f - L_f)\})] \\
&+ \frac{A_{f,1}P_{cd}}{\beta_{f,1}} [(\cos\{\beta_{f,1}\bar{x}_f\} + \cosh\{\beta_{f,1}\bar{x}_f\}) (\sin\{\beta_{f,1}\bar{x}_f\} - \sin\{\beta_{f,1}(\bar{x}_f - L_f)\}) - \sinh\{\beta_{f,1}\bar{x}_f\} + \sinh\{\beta_{f,1}(\bar{x}_f - L_f)\})] \\
&+ (P_{cU} - P_{cL}) L_c A_{f,1} [(\sin\beta_{f,1}\bar{x}_f - \sinh\beta_{f,1}\bar{x}_f) (\sin\beta_{f,1}x_{canard} - \sinh\beta_{f,1}x_{canard}) + (\cos\beta_{f,1}\bar{x}_f + \cosh\beta_{f,1}\bar{x}_f) (\cos\beta_{f,1}x_{canard} - \cosh\beta_{f,1}x_{canard})] \\
&\hspace{15em} (112) \\
N_{a,1}(t) &= \frac{2A_{a,1}P_{cf}}{\beta_{a,1}} (\sin\beta_{a,1}\bar{x}_a - \sinh\beta_{a,1}\bar{x}_a) \\
&+ A_{a,1}C_1C_3 \left[ \frac{1}{\beta_{a,1}^2} \sin\beta_{a,1}\bar{x}_a - \frac{\bar{x}_a}{\beta_{a,1}} \cos\beta_{a,1}\bar{x}_a - \frac{1}{\beta_{a,1}^2} \sin(\beta_{a,1}(\bar{x}_a - L_a)) + \frac{\bar{x}_a - L_a}{\beta_{a,1}} \cos(\beta_{a,1}(\bar{x}_a - L_a)) \right] \\
&\quad + \frac{A_{a,1}C_1C_4}{\beta_{a,1}} [\cos\beta_{a,1}\bar{x}_a - \cos(\beta_{a,1}(\bar{x}_a - L_a))] \\
&+ A_{a,1}C_1C_3 \left[ \frac{-\bar{x}_a}{\beta_{a,1}} \cosh\beta_{a,1}\bar{x}_a + \frac{1}{\beta_{a,1}^2} \sinh\beta_{a,1}\bar{x}_a + \frac{1}{\beta_{a,1}} (\bar{x}_a - L_a) \cosh(\beta_{a,1}(\bar{x}_a - L_a)) - \frac{1}{\beta_{a,1}^2} \sinh(\beta_{a,1}(\bar{x}_a - L_a)) \right] \\
&\quad + \frac{A_{a,1}C_1C_4}{\beta_{a,1}} [\cosh\beta_{a,1}\bar{x}_a - \cosh(\beta_{a,1}(\bar{x}_a - L_a))] \\
&+ A_{a,1}C_2C_3 \left[ \frac{1}{\beta_{a,1}^2} \cos\beta_{a,1}\bar{x}_a + \frac{\bar{x}_a}{\beta_{a,1}} \sin\beta_{a,1}\bar{x}_a - \frac{1}{\beta_{a,1}^2} \cos(\beta_{a,1}(\bar{x}_a - L_a)) - \frac{\bar{x}_a - L_a}{\beta_{a,1}} \sin(\beta_{a,1}(\bar{x}_a - L_a)) \right] \\
&\quad - \frac{A_{a,1}C_2C_4}{\beta_{a,1}} [\sin\beta_{a,1}\bar{x}_a - \sin(\beta_{a,1}(\bar{x}_a - L_a))] \\
&+ A_{a,1}C_2C_3 \left[ \frac{-\bar{x}_a}{\beta_{a,1}} \sinh\beta_{a,1}\bar{x}_a + \frac{1}{\beta_{a,1}^2} \cosh\beta_{a,1}\bar{x}_a + \frac{(\bar{x}_a - L_a)}{\beta_{a,1}} \sinh(\beta_{a,1}(\bar{x}_a - L_a)) - \frac{1}{\beta_{a,1}^2} \cosh(\beta_{a,1}(\bar{x}_a - L_a)) \right] \\
&\quad + \frac{A_{a,1}C_2C_4}{\beta_{a,1}} [\sin\beta_{a,1}\bar{x}_a - \sinh(\beta_{a,1}(\bar{x}_a - L_a))] \\
&+ A_{a,1} (P_{eU} - P_{eL}) L_e [(\sin\beta_{a,1}\bar{x}_a - \sinh\beta_{a,1}\bar{x}_a) (\sin\beta_{a,1}x_{elev} - \sinh\beta_{a,1}x_{elev}) + (\cos\beta_{a,1}\bar{x}_a + \cosh\beta_{a,1}\bar{x}_a) (\cos\beta_{a,1}x_{elev} - \cosh\beta_{a,1}x_{elev})] \\
&\hspace{15em} (113)
\end{aligned}$$

where

$$\begin{aligned}
C_1 &= \sin\beta_{a,1}\bar{x}_a - \sinh\beta_{a,1}\bar{x}_a \\
C_2 &= \cos\beta_{a,1}\bar{x}_a + \cosh\beta_{a,1}\bar{x}_a \\
C_3 &= \frac{P_\infty - P_e}{-L_a} \\
C_4 &= C_3 (L_a - \bar{x}_a) - P_e
\end{aligned} \tag{114}$$

From Eq. 97

$$\begin{aligned}
\frac{\partial C_M}{\partial \dot{\eta}_{f,1}} = & \frac{2A_{f,1}\rho_{cf}a_{cf} \sin \tau_{1,U} \tan \tau_{1,U}}{\beta_{f,1}^2 q_{\infty} S \bar{c}} [1 - \cos \beta_{f,1} \bar{x}_f + \cos \beta_{f,1} \bar{x}_f \cosh \beta_{f,1} \bar{x}_f - \cosh \beta_{f,1} \bar{x}_f - \bar{x}_f \beta_{f,1} (\sin \beta_{f,1} \bar{x}_f - \sinh \beta_{f,1} \bar{x}_f)] \\
& + \frac{A_{f,1}\rho_{cd}a_{cd} \sin \tau_{1,L} \tan \tau_{1,L}}{\beta_{f,1}^2 q_{\infty} S \bar{c}} [2 - \cos \beta_{f,1} L_f + \beta_{f,1} (\bar{x}_f - L_f) \sin \beta_{f,1} L_f + 2 \cos \beta_{f,1} \bar{x}_f \cosh \beta_{f,1} \bar{x}_f] \\
& + \frac{A_{f,1}\rho_{cd}a_{cd} \sin \tau_{1,L} \tan \tau_{1,L}}{\beta_{f,1}^2 q_{\infty} S \bar{c}} [\beta_{f,1} (\bar{x}_f - L_f) (\sin \beta_{f,1} \bar{x}_f \cosh \beta_{f,1} (\bar{x}_f - L_f) + \cos \beta_{f,1} \bar{x}_f \sinh \beta_{f,1} (\bar{x}_f - L_f))] \\
& + \frac{A_{f,1}\rho_{cd}a_{cd} \sin \tau_{1,L} \tan \tau_{1,L}}{\beta_{f,1}^2 q_{\infty} S \bar{c}} [-\sin \beta_{f,1} \bar{x}_f \sinh \beta_{f,1} (\bar{x}_f - L_f) - \cos \beta_{f,1} \bar{x}_f \cosh \beta_{f,1} (\bar{x}_f - L_f)] \\
& + \frac{A_{f,1}\rho_{cd}a_{cd} \sin \tau_{1,L} \tan \tau_{1,L}}{\beta_{f,1}^2 q_{\infty} S \bar{c}} [\sinh \beta_{f,1} \bar{x}_f \sin \beta_{f,1} (\bar{x}_f - L_f) - \cosh \beta_{f,1} \bar{x}_f \cos \beta_{f,1} (\bar{x}_f - L_f)] \\
& + \frac{A_{f,1}\rho_{cd}a_{cd} \sin \tau_{1,L} \tan \tau_{1,L}}{\beta_{f,1}^2 q_{\infty} S \bar{c}} [-\beta_{f,1} (\bar{x}_f - L_f) \sinh \beta_{f,1} \bar{x}_f \cos \beta_{f,1} (\bar{x}_f - L_f) - \beta_{f,1} (\bar{x}_f - L_f) \cosh \beta_{f,1} \bar{x}_f \sin \beta_{f,1} (\bar{x}_f - L_f)] \\
& + \frac{A_{f,1}\rho_{cd}a_{cd} \sin \tau_{1,L} \tan \tau_{1,L}}{\beta_{f,1}^2 q_{\infty} S \bar{c}} [-\beta_{f,1} (\bar{x}_f - L_f) \sinh \beta_{f,1} L_f - \cosh \beta_{f,1} L_f] \\
& - \frac{A_{f,1}\rho_{cd}a_{cd} \sin \tau_{1,L} \tan \tau_{1,L} \bar{x}_f}{\beta_{f,1} q_{\infty} S \bar{c}} [(\sin \beta_{f,1} \bar{x}_f - \sinh \beta_{f,1} \bar{x}_f) (\cos \beta_{f,1} (\bar{x}_f - L_f) + \cosh \beta_{f,1} (\bar{x}_f - L_f))] \\
& - \frac{A_{f,1}\rho_{cd}a_{cd} \sin \tau_{1,L} \tan \tau_{1,L} \bar{x}_f}{\beta_{f,1} q_{\infty} S \bar{c}} [(\cos \beta_{f,1} \bar{x}_f + \cosh \beta_{f,1} \bar{x}_f) (-\sin \beta_{f,1} (\bar{x}_f - L_f) + \sinh \beta_{f,1} (\bar{x}_f - L_f))] \\
& + \frac{2A_{f,1}\rho_{cf}a_{cf} \cos \tau_{1,U}}{\beta_{f,1}^2 q_{\infty} S \bar{c}} [1 - \cos \beta_{f,1} \bar{x}_f + \cos \beta_{f,1} \bar{x}_f \cosh \beta_{f,1} \bar{x}_f - \cosh \beta_{f,1} \bar{x}_f] \\
& + \frac{A_{f,1}\rho_{cd}a_{cd} \cos \tau_{1,L}}{\beta_{f,1}^2 q_{\infty} S \bar{c}} [2 - \cos \beta_{f,1} L_f + \beta_{f,1} (\bar{x}_f - L_f) \sin \beta_{f,1} L_f + 2 \cos \beta_{f,1} \bar{x}_f \cosh \beta_{f,1} \bar{x}_f] \\
& + \frac{A_{f,1}\rho_{cd}a_{cd} \cos \tau_{1,L}}{\beta_{f,1}^2 q_{\infty} S \bar{c}} [\beta_{f,1} (\bar{x}_f - L_f) (\sin \beta_{f,1} \bar{x}_f \cosh \beta_{f,1} (\bar{x}_f - L_f) + \cos \beta_{f,1} \bar{x}_f \sinh \beta_{f,1} (\bar{x}_f - L_f))] \\
& + \frac{A_{f,1}\rho_{cd}a_{cd} \cos \tau_{1,L}}{\beta_{f,1}^2 q_{\infty} S \bar{c}} [-\sin \beta_{f,1} \bar{x}_f \sinh \beta_{f,1} (\bar{x}_f - L_f) - \cos \beta_{f,1} \bar{x}_f \cosh \beta_{f,1} (\bar{x}_f - L_f)] \\
& + \frac{A_{f,1}\rho_{cd}a_{cd} \cos \tau_{1,L}}{\beta_{f,1}^2 q_{\infty} S \bar{c}} [\sinh \beta_{f,1} \bar{x}_f \sin \beta_{f,1} (\bar{x}_f - L_f) - \cosh \beta_{f,1} \bar{x}_f \cos \beta_{f,1} (\bar{x}_f - L_f)] \\
& + \frac{A_{f,1}\rho_{cd}a_{cd} \cos \tau_{1,L}}{\beta_{f,1}^2 q_{\infty} S \bar{c}} [-\beta_{f,1} (\bar{x}_f - L_f) \sinh \beta_{f,1} \bar{x}_f \cos \beta_{f,1} (\bar{x}_f - L_f) - \beta_{f,1} (\bar{x}_f - L_f) \cosh \beta_{f,1} \bar{x}_f \sin \beta_{f,1} (\bar{x}_f - L_f)] \\
& + \frac{A_{f,1}\rho_{cd}a_{cd} \cos \tau_{1,L}}{\beta_{f,1}^2 q_{\infty} S \bar{c}} [-\beta_{f,1} (\bar{x}_f - L_f) \sinh \beta_{f,1} L_f - \cosh \beta_{f,1} L_f]
\end{aligned} \tag{115}$$

From Eq. 98

$$\begin{aligned}
\frac{\partial C_Z}{\partial \dot{\eta}_{a,1}} &= \frac{-2\rho_{cf}a_{cf} \cos(\tau_{1,U} + \tau_2) A_{a,1}}{q_\infty S \beta_{a,1}} [\sin \beta_{a,1} \bar{x}_a - \sinh \beta_{a,1} \bar{x}_a] \\
&\quad - \frac{1}{q_\infty S \beta_{a,1}} [(f_1 \bar{x}_a^2 + g_1 \bar{x}_a + h_1) \cos \beta_{a,1} \bar{x}_a + (f_1 k_1^2 + g_1 k_1 + h_1) \cos(\beta_{a,1} k_1)] \\
&\quad + \frac{1}{q_\infty S \beta_{a,1}^2} (2f_1 \bar{x}_a + g_1) \sin \beta_{a,1} \bar{x}_a - \frac{2f_1 k_1 + g_1}{q_\infty S \beta_{a,1}} \sin \beta_{a,1} k_1 + \frac{2f_1}{q_\infty S \beta_{a,1}^3} (\cos \beta_{a,1} \bar{x}_a - \cos \beta_{a,1} k_1) \\
&\quad - \frac{1}{q_\infty S \beta_{a,1}} \left[ (f_1 \bar{x}_a^2 + g_1 \bar{x}_a + h_1) \cosh \beta_{a,1} \bar{x}_a - \frac{1}{\beta_{a,1}} (2f_1 \bar{x}_a + g_1) \sinh \beta_{a,1} \bar{x}_a + \frac{2f_1}{\beta_{a,1}^2} \cosh \beta_{a,1} \bar{x}_a \right] \\
&\quad + \frac{1}{q_\infty S \beta_{a,1}} \left[ (f_1 k_1^2 + g_1 k_1 + h_1) \cosh \beta_{a,1} k_1 - \frac{1}{\beta_{a,1}} (2f_1 k_1 + g_1) \sinh \beta_{a,1} k_1 + \frac{2f_1}{\beta_{a,1}^2} \cosh \beta_{a,1} k_1 \right] \quad (116) \\
&\quad + \frac{1}{q_\infty S \beta_{a,1}} \left[ (f_1 \bar{x}_a^2 + g_1 \bar{x}_a + h_1) \sin \beta_{a,1} \bar{x}_a + \frac{1}{\beta_{a,1}} (2f_1 \bar{x}_a + g_1) \cos \beta_{a,1} \bar{x}_a - \frac{1}{\beta_{a,1}} 2f_1 \sin \beta_{a,1} \bar{x}_a \right] \\
&\quad - \frac{1}{q_\infty S \beta_{a,1}} \left[ (f_1 k_1^2 + g_1 k_1 + h_1) \sin \beta_{a,1} k_1 + \frac{1}{\beta_{a,1}} (2f_1 k_1 + g_1) \cos \beta_{a,1} k_1 - \frac{1}{\beta_{a,1}} 2f_1 \sin \beta_{a,1} k_1 \right] \\
&\quad + \frac{1}{q_\infty S \beta_{a,1}} \left[ - (f_1 \bar{x}_a^2 + g_1 \bar{x}_a + h_1) \sinh \beta_{a,1} \bar{x}_a + \frac{1}{\beta_{a,1}} (2f_1 \bar{x}_a + g_1) \cosh \beta_{a,1} \bar{x}_a - \frac{1}{\beta_{a,1}} 2f_1 \sinh \beta_{a,1} \bar{x}_a \right] \\
&\quad + \frac{1}{q_\infty S \beta_{a,1}} \left[ - (f_1 k_1^2 + g_1 k_1 + h_1) \sinh \beta_{a,1} k_1 + \frac{1}{\beta_{a,1}} (2f_1 k_1 + g_1) \cosh \beta_{a,1} k_1 - \frac{1}{\beta_{a,1}} 2f_1 \sinh \beta_{a,1} k_1 \right]
\end{aligned}$$

where

$$\begin{aligned}
k_1 &= \bar{x}_a - L_a \\
f_1 &= \rho_a a_a (\sin \beta_{a,1} \bar{x}_a - \sinh \beta_{a,1} \bar{x}_a) \\
g_1 &= (\sin \beta_{a,1} \bar{x}_a - \sinh \beta_{a,1} \bar{x}_a) (-a_a \rho_a \{L_a - \bar{x}_a\} + a_a \rho_e) (-a_a \rho_a \{L_a - \bar{x}_a\} + a_e \rho_a) \\
h_1 &= (\sin \beta_{a,1} \bar{x}_a - \sinh \beta_{a,1} \bar{x}_a) (-\rho_a \{L_a - \bar{x}_a\} + \rho_e) (-a_a \{L_a - \bar{x}_a\} + a_e) \\
\rho_a &= \frac{\rho_\infty - \rho_e}{-L_a} \\
a_a &= \frac{a_\infty - a_e}{-L_a}
\end{aligned} \quad (117)$$



Continued from Eq. 99

$$\begin{aligned}
\frac{\partial C_M}{\partial \dot{\eta}_{a,1 P2}} &= \frac{\rho_a a_a \cos(\tau_{1,U} + \tau_2)}{q_\infty S \bar{c}} A_{a,1} (\sin \beta_{a,1} \bar{x}_a - \sinh \beta_{a,1} \bar{x}_a) \left[ \frac{3\beta_{a,1}^2 \bar{x}_a^2 - 6}{\beta_{a,1}^4} \sin \beta_{a,1} \bar{x}_a - \frac{\beta_{a,1}^2 \bar{x}_a^3 - 6\bar{x}_a}{\beta_{a,1}^3} \cos \beta_{a,1} \bar{x}_a \right] \\
&- \frac{\rho_a a_a \cos(\tau_{1,U} + \tau_2)}{q_\infty S \bar{c}} A_{a,1} (\sin \beta_{a,1} \bar{x}_a - \sinh \beta_{a,1} \bar{x}_a) \left[ \frac{3\beta_{a,1}^2 (\bar{x}_a - L_a)^2 - 6}{\beta_{a,1}^4} \sin \beta_{a,1} (\bar{x}_a - L_a) - \frac{\beta_{a,1}^2 (\bar{x}_a - L_a)^3 - 6(\bar{x}_a - L_a)}{\beta_{a,1}^3} \cos \beta_{a,1} (\bar{x}_a - L_a) \right] \\
&+ \frac{\rho_a a_a \cos(\tau_{1,U} + \tau_2)}{q_\infty S \bar{c}} A_{a,1} (\sin \beta_{a,1} \bar{x}_a - \sinh \beta_{a,1} \bar{x}_a) \left[ -\frac{1}{\beta_{a,1}^4} (\beta_{a,1}^3 \bar{x}_a^3 \cosh \beta_{a,1} \bar{x}_a - 3\beta_{a,1}^2 \bar{x}_a^2 \sinh \beta_{a,1} \bar{x}_a + 6\beta_{a,1} \bar{x}_a \cosh \beta_{a,1} \bar{x}_a - 6 \sinh \beta_{a,1} \bar{x}_a) \right] \\
&\quad + \frac{\rho_a a_a \cos(\tau_{1,U} + \tau_2)}{q_\infty S \bar{c}} A_{a,1} (\sin \beta_{a,1} \bar{x}_a - \sinh \beta_{a,1} \bar{x}_a) * \\
&* \left[ \frac{1}{\beta_{a,1}^4} (\beta_{a,1}^3 (\bar{x}_a - L_a)^3 \cosh \beta_{a,1} (\bar{x}_a - L_a) - 3\beta_{a,1}^2 (\bar{x}_a - L_a)^2 \sinh \beta_{a,1} (\bar{x}_a - L_a) + 6\beta_{a,1} (\bar{x}_a - L_a) \cosh \beta_{a,1} (\bar{x}_a - L_a) - 6 \sinh \beta_{a,1} (\bar{x}_a - L_a)) \right] \\
&\quad + \frac{\rho_a a_a \cos(\tau_{1,U} + \tau_2)}{q_\infty S \bar{c}} A_{a,1} (\cos \beta_{a,1} \bar{x}_a - \cosh \beta_{a,1} \bar{x}_a) \left[ \frac{3\beta_{a,1}^2 \bar{x}_a^2 - 6}{\beta_{a,1}^4} \cos \beta_{a,1} \bar{x}_a - \frac{\beta_{a,1}^2 \bar{x}_a^3 - 6\bar{x}_a}{\beta_{a,1}^3} \sin \beta_{a,1} \bar{x}_a \right] \\
&- \frac{\rho_a a_a \cos(\tau_{1,U} + \tau_2)}{q_\infty S \bar{c}} A_{a,1} (\cos \beta_{a,1} \bar{x}_a - \cosh \beta_{a,1} \bar{x}_a) \left[ \frac{3\beta_{a,1}^2 (\bar{x}_a - L_a)^2 - 6}{\beta_{a,1}^4} \cos \beta_{a,1} (\bar{x}_a - L_a) - \frac{\beta_{a,1}^2 (\bar{x}_a - L_a)^3 - 6(\bar{x}_a - L_a)}{\beta_{a,1}^3} \sin \beta_{a,1} (\bar{x}_a - L_a) \right] \\
&\quad + \frac{\rho_a a_a \cos(\tau_{1,U} + \tau_2)}{q_\infty S \bar{c}} A_{a,1} (\cos \beta_{a,1} \bar{x}_a - \cosh \beta_{a,1} \bar{x}_a) \left[ \frac{-1}{\beta_{a,1}^4} (\beta_{a,1}^3 \bar{x}_a^3 \sinh \beta_{a,1} \bar{x}_a - 3\beta_{a,1}^2 \bar{x}_a^2 \cosh \beta_{a,1} \bar{x}_a + 6\beta_{a,1} \bar{x}_a \sinh \beta_{a,1} \bar{x}_a - 6 \cosh \beta_{a,1} \bar{x}_a) \right] \\
&\quad - \frac{\rho_a a_a \cos(\tau_{1,U} + \tau_2)}{q_\infty S \bar{c}} A_{a,1} (\cos \beta_{a,1} \bar{x}_a - \cosh \beta_{a,1} \bar{x}_a) * \\
&* \left[ \frac{-1}{\beta_{a,1}^4} (\beta_{a,1}^3 (\bar{x}_a - L_a)^3 \sinh \beta_{a,1} (\bar{x}_a - L_a) - 3\beta_{a,1}^2 (\bar{x}_a - L_a)^2 \cosh \beta_{a,1} (\bar{x}_a - L_a) + 6\beta_{a,1} (\bar{x}_a - L_a) \sinh \beta_{a,1} (\bar{x}_a - L_a) - 6 \cosh \beta_{a,1} (\bar{x}_a - L_a)) \right] \\
&\quad + \frac{\cos(\tau_{1,U} + \tau_2)}{q_\infty S \bar{c}} J_5 A_{a,1} \left[ \frac{2\bar{x}_a}{\beta_{a,1}^2} \sin \beta_{a,1} \bar{x}_a - \frac{\beta_{a,1} \bar{x}_a^2 - 2}{\beta_{a,1}^3} \cos \beta_{a,1} \bar{x}_a - \left\{ \frac{2(\bar{x}_a - L_a)}{\beta_{a,1}^2} \sin \beta_{a,1} (\bar{x}_a - L_a) - \frac{\beta_{a,1} (\bar{x}_a - L_a)^2 - 2}{\beta_{a,1}^3} \cos \beta_{a,1} (\bar{x}_a - L_a) \right\} \right] \\
&\quad + \frac{\cos(\tau_{1,U} + \tau_2)}{q_\infty S \bar{c}} J_5 A_{a,1} * \\
&* \left[ \beta_{a,1}^2 \bar{x}_a^2 \cosh \beta_{a,1} \bar{x}_a - 2\beta_{a,1} \bar{x}_a \sinh \beta_{a,1} \bar{x}_a + 2 \cosh \beta_{a,1} \bar{x}_a - \left\{ \beta_{a,1}^2 (\bar{x}_a - L_a)^2 \cosh \beta_{a,1} (\bar{x}_a - L_a) - 2\beta_{a,1} (\bar{x}_a - L_a) \sinh \beta_{a,1} (\bar{x}_a - L_a) + 2 \cosh \beta_{a,1} (\bar{x}_a - L_a) \right\} \right] \\
&\quad + \frac{\cos(\tau_{1,U} + \tau_2)}{q_\infty S \bar{c}} J_5 A_{a,1} \left[ \frac{2\bar{x}_a \cos \beta_{a,1} \bar{x}_a}{\beta_{a,1}^2} + \frac{\beta_{a,1}^2 \bar{x}_a^2 - 2}{\beta_{a,1}^3} \sin \beta_{a,1} \bar{x}_a - \left\{ \frac{2(\bar{x}_a - L_a) \cos \beta_{a,1} (\bar{x}_a - L_a)}{\beta_{a,1}^2} + \frac{\beta_{a,1}^2 (\bar{x}_a - L_a)^2 - 2}{\beta_{a,1}^3} \sin \beta_{a,1} (\bar{x}_a - L_a) \right\} \right] \\
&\quad - \frac{\cos(\tau_{1,U} + \tau_2)}{q_\infty S \bar{c}} J_5 A_{a,1} \left[ \beta_{a,1}^2 \bar{x}_a^2 \sinh \beta_{a,1} \bar{x}_a - 2\beta_{a,1} \bar{x}_a \cosh \beta_{a,1} \bar{x}_a + 2 \sinh \beta_{a,1} \bar{x}_a \right] \\
&\quad + \frac{\cos(\tau_{1,U} + \tau_2)}{q_\infty S \bar{c}} J_5 A_{a,1} \left[ \beta_{a,1}^2 (\bar{x}_a - L_a)^2 \sinh \beta_{a,1} (\bar{x}_a - L_a) - 2\beta_{a,1} (\bar{x}_a - L_a) \cosh \beta_{a,1} (\bar{x}_a - L_a) + 2 \sinh \beta_{a,1} (\bar{x}_a - L_a) \right] \\
&+ \frac{\cos(\tau_{1,U} + \tau_2)}{q_\infty S \bar{c}} J_6 A_{a,1} \left[ 2 - \cos \beta_{a,1} L_a + \beta_{a,1} (\bar{x}_a - L_a) \sin \beta_{a,1} L_a + \beta_{a,1} (\bar{x}_a - L_a) \left\{ \sin \beta_{a,1} \bar{x}_a \cosh \beta_{a,1} (\bar{x}_a - L_a) + \cos \beta_{a,1} \bar{x}_a \sinh \beta_{a,1} (\bar{x}_a - L_a) \right\} \right] \\
&\quad + \frac{\cos(\tau_{1,U} + \tau_2)}{q_\infty S \bar{c}} J_6 A_{a,1} \left[ 2 \cos \beta_{a,1} \bar{x}_a \cosh \beta_{a,1} \bar{x}_a - \sin \beta_{a,1} \bar{x}_a \sinh \beta_{a,1} (\bar{x}_a - L_a) - \cos \beta_{a,1} \bar{x}_a \cosh \beta_{a,1} (\bar{x}_a - L_a) + \sin \beta_{a,1} (\bar{x}_a - L_a) \sinh \beta_{a,1} \bar{x}_a \right] \\
&\quad + \frac{\cos(\tau_{1,U} + \tau_2)}{q_\infty S \bar{c}} J_6 A_{a,1} \left[ -\cos \beta_{a,1} (\bar{x}_a - L_a) \cosh \beta_{a,1} \bar{x}_a - \beta_{a,1} (\bar{x}_a - L_a) \cos \beta_{a,1} (\bar{x}_a - L_a) \sinh \beta_{a,1} \bar{x}_a \right] \\
&\quad + \frac{\cos(\tau_{1,U} + \tau_2)}{q_\infty S \bar{c}} J_6 A_{a,1} \left[ -\beta_{a,1} (\bar{x}_a - L_a) \sin \beta_{a,1} (\bar{x}_a - L_a) \cosh \beta_{a,1} \bar{x}_a - \beta_{a,1} (\bar{x}_a - L_a) \sinh \beta_{a,1} L_a - \cosh \beta_{a,1} L_a \right] \\
\end{aligned} \tag{119}$$

where

$$\begin{aligned}
\frac{\partial C_M}{\partial \dot{\eta}_{a,1}} &= \frac{\partial C_M}{\partial \dot{\eta}_{a,1 P1}} + \frac{\partial C_M}{\partial \dot{\eta}_{a,1 P2}} \tag{120} \\
J_1 &= \rho_a a_a m_1 \\
J_2 &= -2k\rho_a a_a m_1 + \rho_a a_a \{m_1 \bar{x}_a + m_2\} + \{\rho_e a_a + \rho_a a_e\} m_1 \\
J_3 &= \rho_a a_a m_1 k^2 - 2k\rho_a a_a \{m_1 \bar{x}_a + m_2\} - \{\rho_e a_a + \rho_a a_e\} m_1 k + \{\rho_e a_a + \rho_a a_e\} \{m_1 \bar{x}_a + m_2\} + \rho_e a_e m_1 \\
J_4 &= \rho_a a_a \{m_1 \bar{x}_a + m_2\} k^2 - \{\rho_e a_a + \rho_a a_e\} \{m_1 \bar{x}_a + m_2\} k + \rho_e a_e \{m_1 \bar{x}_a + m_2\} \\
J_5 &= 2k\rho_a a_a + (\rho_e a_a + \rho_a a_e) \\
J_6 &= \rho_a a_a k^2 - k(\rho_e a_a \rho_a a_e) + \rho_e a_e \\
\rho_a &= \frac{\rho_\infty - \rho_e}{-L_a} \\
a_a &= \frac{a_\infty - a_e}{-L_a} \\
k &= L_a - \bar{x}_a \\
m_1 &= \tan(\tau_{1,U} + \tau_2) \\
m_2 &= -L \tan \tau_{1,U} \tag{121}
\end{aligned}$$